NOTICE

The quality of this microform is heavily dependent upon the quality of the original thesis submitted for microfilming. Every effort has been made to ensure the highest quality of reproduction possible.

If pages are missing, contact the university which granted the degree.

Some pages may have indistinct print especially if the original pages were typed with a poor typewriter ribbon or if the university sent us an inferior photocopy.

Reproduction in full or in part of this microform is governed by the Canadian Copyright Act, R.S.C. 1970, c. C-30, and subsequent amendments.

AVIS

La qualité de cette microforme dépend grandement de la qualité de la thèse soumise au microfilmage. Nous avons tout fait pour assurer une qualité supérieure de reproduction.

S'il manque des pages, veuillez communiquer avec l'université qui a conféré le grade.

La qualité d'impression de certaines pages peut laisser à désirer, surtout si les pages originales ont été dactylographiées à l'aide d'un ruban usé ou si l'université nous a fait parvenir une photocopie de qualité inférieure.

La reproduction, même partielle, de cette microforme est soumise à la Loi canadienne sur le droit d'auteur, SRC 1970, c. C-30, et ses amendements subséquents.

EFFECTS OF VISCOSITY ON DYNAMIC INTERFACIAL TENSION

by

Youssef Touhami

A thesis submitted to the School of Graduate Studies
in partial fulfillment of the requirements for the degree of
Master of Applied Science
in
Chemical Engineering

DEPARTMENT OF CHEMICAL ENGINEERING
UNIVERSITY OF OTTAWA

OTTAWA, CANADA, 1990

ISBN 0-315-60077-2

UNIVERSITÉ D'OTTAWA
UNIVERSITY OF OTTAWA

Abstract

In enhanced oil recovery by caustic waterflooding mobility control will have to be provided in order to improve the overall sweep efficiency. For this reason, water-soluble polymers may be added to caustic solutions to enhance bulk viscosity. However, the addition of a polymer may not necessarily improve the interfacial effectiveness of the caustic solution. It is thus desirable to investigate the effect of thickening the caustic solution (by using various polymers) on bulk phase viscosity and dynamic interfacial tension (IFT).

In this study, we have investigated the IFT-lowering potential of a range of caustic solutions which were contacted with dilute solution of linoleic acid in light paraffin oil. Two polymers, namely, polyvinyl alcohol and polyacrylamide were added to the caustic solution in order to increase bulk phase viscosity. The dynamic IFT of caustic, polymer and caustic-polymer solutions were measured. By using different linoleic acid concentrations up to 100 mM, it was found that an increase in acid concentration was accompanied by a decrease in IFT for any given caustic composition. When the acid strength was fixed at 10 mM and the caustic concentration was also increased up maximum of 250 mM, the lowest IFT values were obtained at 12.5 mM NaOH.

The addition of polyvinyl alcohol up to 3 % by weight increased the aqueous phase viscosity from 1.0 to 28.0 mPa.s. By adding polyacrylamide to the caustic in an amount not exceeding 0.3 % by weight, the viscosity of the caustic solution was raised to 20 mPa.s. The polymers on their own were found to possess a signifi-

cant interfacial activity compared to neutral water. Generally, the dilute polymer solutions lowered the IFT of the oleic phase against neutral water from 30.0 to about 15 mN/m. However, the addition of the polymeric material to the caustic solution produced a marginal reduction in dynamic IFT at early contact times and also produced characteristic IFT minima at all caustic concentrations. Beyond the minimum, the increase in IFT at longer contact times was more pronounced in the presence of polymer.

Acknowledgements

Special appreciation is expressed to Drs. G. Neale and V. Hornof for their assistance, guidance, and supervision of this project. Also I wish to thank Dr. C.I. Chiwetelu for his invaluable suggestions and advices in the preparation of this thesis.

Sincere appreciation is also expressed to the Tunisian Government for providing scholarship.

Contents

List of Tables

List of Figures

Nomenclature

a	exponent for Mark-Houwink equation
a_i	constant in Flory-Huggin equation
C	molar concentrations
C_p	polymer concentrations g/m^3
D	droplet width
d^*	width dimension from spinning drop tensiometer
f	tractive force pulligng ring
F	correction factor
g	gravitational acceleration
K′	Mark-Houwink constant
K_{ap}	cell constant of the Anton Parr densimeter
K_D	acid distribution ratio water/oil
K_s	equilibrium constant associated with species, NaA
K_{s1}	inactive soap dissociation constant
K_{s2}	inactive soap distribution ratio
K_w	ionic product of water
K_X	acid dissociation constant
L	droplet length
m	power law coefficient
n	power law exponent
P	pressure
r	radius of a sphere of same volume as the drop
R	radius of ring
R_1, R_2	radii of curvature
R_o	radius of curvature at the origin
r^*_{max}	dimensionless parameter defined in Eq. 3.4
T	period of revolution (msec/rev)
V	droplet volume
y	distance measured in the direction perpendicular to the axis of rotation
y_o	droplet width
z	distance measured along the axis of symmetry of pendant drop

SUBSCRIPTS

HL	linoleic acid
HX	acid species
i	phase identity
NaX	inactive soap species or salt
o	initial state, oleic phase
PAM	polyvinyl alcohol
PS	polystyrene
PVA	polyacrylamide
s	sublayer
w	water, aqueous phase
X	surfactant

GREEK LETTERS

γ	interfacial tension, mN/m
γ_{ap}	apparent interfacial tension from ring tensiometer
γ_t	true interfacial tension from ring tensiometer
$\dot{\gamma}$	shear rate, s^{-1}
μ	viscosity of polymer solution, mPa.s
μ_1	brine viscosity
$[\mu]$	intrinsic viscosity
ω	angular velocity (rad/sec)
ρ	density

Chapter 1

Introduction

1.1 The Nature of Dynamic Interfacial Tension

Dynamic interfacial tension is a phenomenon which is often associated with the transfer of surface active materials between two immiscible liquid phases which are in contact. The surface active material is originally present in one of the liquid phases, but when the two phases are brought into contact, there is a tendency for some of the surfactant molecules to diffuse to the other liquid phase in which it was originally absent. Ordinarily, this diffusion of surfactant molecules would be expected to be governed by the law of unsteady-state mass transfer until an equilibrium is established in the respective bulk fluids.

However, surfactants by their very nature, tend to adsorb and accumulate at the interface separating the two bulk phases. The rate of adsorption is governed by the amount of surfactant already adsorbed and by the presence of any barriers

to the removal of adsorbed species from the interface. Thus, the entire adsorption process is time-dependent. Consequently, the prevailing interfacial tension remains strongly time-dependent until an equilibrium condition is attained. This so-called dynamic interfacial tension plays a considerable role in liquid-liquid extraction, and chemical enhanced oil recovery. In the case of the latter, reacting species in the form of carboxylic acids are originally present in the crude oil. The injection of an alkaline floodwater into the reservoir enables water-borne bases to contact and to react with the acids present in the oleic phase. The result is the in-situ formation of surface-active soaps which are responsible for the dramatic reduction in oil-water interfacial tension as well as the dynamic nature of such interfacial tension. Sherwood and Wei [1] have shown that the transfer of solutes between immiscible solvents is strongly influenced by the presence of adsorption barriers particularly when surface reactions are involved. However, it was left to England and Berg [2] and later Rubin and Radke [3] to relate quantitatively the effect of these interfacial barriers on the rate of accumulation and hence on the magnitude of dynamic interfacial tension.

1.2 Bulk Phase Viscosity and Dynamic IFT

Traditionally, the development of theories and experimental procedures for the measurement of interfacial tension has relied heavily on thermodynamic principles. Indeed, the very concept of interfacial tension presupposes the existence of thermo-

dynamic equilibrium between the two liquid phases. Adamson [4] and Davies and Rideal [5] have summarized the various methods which are currently in use for interfacial tension measurement. These methods fall into two broad classes, namely;

(i) Those based on equilibrium at the boundary of static droplets.

(ii) Those based on forces at equilibrium on the surface of droplets rotating at constant angular velocity.

The governing equations for both situations, originally due to Young and Laplace [4,6], can be stated as follows:

$$\Delta P = \gamma \left(\frac{1}{R_1} + \frac{1}{R_2} \right). \tag{1.1}$$

For a stagnant system involving a static droplet, Bashforth and Adams [7] have shown that a balance between capillary and buoyancy forces requires that the following relationship holds, viz:

$$\Delta P = \gamma \left(\frac{1}{R_1} + \frac{1}{R_2} \right) = \frac{2\gamma}{R_o} + \Delta \rho g z. \tag{1.2}$$

In the case of spinning drop tensiometry [8,9], the forces at balance on the surface of a rotating oil droplet are as follows:

$$\Delta P = \gamma \left(\frac{1}{R_1} + \frac{1}{R_2} \right) = \frac{2\gamma}{R_o} - \frac{\Delta \rho \omega^2 y^2}{2}. \tag{1.3}$$

In all these three fundamental equations, the influence of viscosity is conspicuously absent. Current methods for the measurement of dynamic interfacial tension are based on those same equations. It is therefore not surprising that the influence

of viscosity on dynamic interfacial tension cannot be readily quantified. Work by Rubin and Radke [3] showed that changing the viscosity of the oleic phase produced a marked difference in the values of dynamic interfacial tensions. Neale et al. [10] used a diluted Lloydminster crude oil in toluene as the constitutive oil but altered its viscosity by adding increasing amounts of polystyrene. Their results showed that as the oleic phase became more viscous, the apparent dynamic interfacial tension was progressively lowered while interfacial tension-time trends remained largely unchanged. The authors argued that the increased oleic phase viscosity dampened the extent of contraction and elongation of the spinning oil droplet and thereby led to smaller apparent interfacial tension values.

1.3 Objective of this Study

From a practical enhanced oil recovery perspective, it would be desirable to decrease the viscosity of the crude oil in order to prevent excessive fingering of the displacing aqueous phase. This can be achieved by direct or indirect heating of the reservoir which is understandably very expensive and often uneconomical. The other option (which is more readily applicable to conventional reservoirs) is to increase the viscosity of the injected phase by the incorporation of polymeric materials. In this work, we have used two such water-soluble polymers, namely polyacrylamide and polyvinyl alcohol to increase the viscosity of aqueous caustic solutions, while leaving the oleic phase viscosity relatively unchanged. The aim is to determine the

extent to which the aqueous phase viscosity can be improved by the addition of a controlled amount of polymers. Additionally, the optimum linoleic acid concentration that produces the maximum interfacial activity against a spectrum of NaOH concentrations was determined. We have studied the interfacial activity associated with the polymeric material. More importantly, we have investigated the effect on dynamic interfacial tension of the incorporation of these polymers at various NaOH concentrations. It is hoped that the results of this work will provide further insight into the formulation and interfacial behavior of caustic solutions that have been thickened with polymeric agents.

Chapter 2

Literature Survey

2.1 Oil Recovery Processes

Over a period of many million years, water, oil, and gas have accumulated in some underground porous rocks, and have separated into fairly distinct layers due to gravity effects. The crude oil is trapped in the pores of the rock by natural forces resulting from viscosity, interfacial tension, and capillarity. Oil recovery from underground reservoirs involves the displacement of the oil from the interstices of the porous rock into the well-bore of production wells. This process requires energy which may be available in the reservoir in the form of dissociated gas coming out of solution, or water encroaching from an adjoining aquifer. Upon drilling the well, the natural driving forces ensure a continuous oil production for several months or years. This process is referred to as "primary recovery" and the oil recovery achieved is quite low, usually 20 to 40% of the original oil-in-place [11,12]. As the oil is produced, the natural reservoir energy is depleted to the point where

there is not sufficient force to drive the oil to the surface. Customarily, however, a fluid such as gas or water is injected into the reservoir to displace the oil, and this process is referred to as "secondary recovery". The resulting oil recovery by this secondary waterflooding is low, only an additional 5 to 10% recovery of the original oil-in-place is achieved [13] and this is due to the chemical and physical properties of the water, and particularly to the large capillary forces trapping the oil in the reservoir matrix. The remaining 60 to 70% oil can often be produced by various other methods, collectively known as "tertiary recovery" processes or "enhanced oil recovery" techniques [13,14]. Enhanced oil recovery processes include:
(i) Chemical processes, (ii) Solvent processes and (iii) Thermal recovery.

2.1.1 Chemical Flooding

Chemical flooding is the most widely used process for typical reservoirs and is comprised of three different types of flooding.

1. Polymer flooding,
2. Micellar-polymer injection,
3. Alkaline flooding.

Polymer Flooding

Polymer flooding consists of adding polymers to the water of a waterflood to decrease its mobility. The resulting increase in viscosity , as well as a decrease in aqueous phase permeability that occurs with some polymers, causes a lower mobility ratio. This thickened water is also used in secondary recovery in order to increase the efficiency of the waterflood through greater volumetric sweep efficiency and a lower swept-zone oil saturation. Generally, a polymer flood is specially developed for application to reservoirs containing low to medium viscosity crude. This polymer process will be economic only when the waterflood mobility is high, when the heterogeneity is high, or when a combination of these two occurs.

Micellar-Polymer Injection

Micellar flooding is the most important process, in that research is based on the improvement of surfactant efficiency in producing more oil. A micellar process is any process that injects surface-active agents (surfactants) to overcome the large capillary forces trapping the oil. Petroleum sulfonates are the most widely used surfactants. The efficacy of this process can be greatly improved by injecting a polymer solution immediately after the surfactant slug, giving the so-called micellar-polymer process.

Alkaline Flooding

Generally, crude oils contain significant amounts of carboxylic acids and other reactive agents. In contrast to micellar-polymer flooding, surfactants in alkaline process are generated in-situ by the reaction between the acids in the crude and the caustic reagents usually added to the flood water. Sodium hydroxide, sodium silicate, and sodium carbonate are the most widely used alkaline chemicals. Oil recovery mechanisms in alkaline flooding have been attributed to interfacial tension lowering, wettability reversal, and emulsion formation.

2.1.2 Solvent Flooding

One of the earliest methods for producing additional oil was through the use of solvents to extract the oil from the permeable media. However this process has become economically less attractive because of an increasing solvent cost. The most widely used solvent is carbon dioxide. Solvent flooding refers to enhanced oil recovery processes in which the main oil recovery mechanism is due to extraction, dissolution, vaporization, solubilization, condensation, or some other phase behavior change involving the crude. The most important oil recovery mechanism is extraction. This oil extraction can be brought about by many fluids: organic alcohols, ketone, refined hydrocarbons, condensed petroleum gas, natural gas and liquified natural gas, carbon dioxide, air, nitrogen and others. Basically, solvent

recovery includes two processes, miscible and immiscible flooding, corresponding to whether or not the solvent develops miscibility with the oil. In general, these processes involved, the same basic recovery mechanisms, which consist particularly of oil viscosity reduction, oil swelling, and solution gas. A typical recovery of 5–15 % can be achieved by this process [11]

2.1.3 Thermal Recovery

Heavy oils are characterized by high viscosity at reservoir conditions, therefore, a successful recovery of heavy oil is dependent on the choice of an appropriate enhanced oil recovery process. To initiate flow of heavy oil, thermal processes are invariably utilized. In these processes, heat is applied to the reservoir in order to raise the temperature of the rock and reservoir fluids. As a result of this temperature increase, the crude oil viscosity is greatly reduced and oil recovery is improved. The most commonly employed thermal techniques are hot water flooding, steam injection and in-situ combustion. Frequently, additives such as alcohol, carbon dioxide and surfactants are injected simultaneously with the steam, in order to reduce the initial oil viscosity and thus improve the injectability of the steam.

2.2 Crude Oil Chemistry

Crude oil is known to contain naturally occurring acidic components. These acids have to be identified with certainty and especially those responsible for the formation of surface active soap molecules by the interaction with alkali in flood water. Some work has been done in this area. Neumann [15] reported that phenols were the main interfacially active constituents of a West German crude oil. Lochte [16] stated that both phenols, and fatty acids of small and long chain aliphatic components, were present. Early work by Seifert and Howells [17] working with Midway Sunset oil from California, suggested that the polar constituents of the oil were responsible for its high interfacial activity. Further, they isolated these polar components into carboxylic, and phenolic fractions. The carboxylic acids were the most dominant interfacially active component and were saturated aliphatics with molecular weight in the 300–400 range. Seifert and Teeter [18,19] and Seifert et al. [20] identified also mono-cyclic and poly-cyclic naphthenic acids as well as aromatic components. Jenkins [21] also isolated cyclic monocarboxylic and fatty acids as well as aliphatic esters from petroleum distillates and from the residues of several crudes.

Jang et al. [22] separated a Long Beach crude oil into various fractions and showed that the interfacial activity with alkali was due to an asphalt-like solid. A further analysis by gas chromatograph and mass spectroscopy identified various long chain carboxylic acids, confirming the views of Seifert and Howells [17] and

Seifert et al. [20], and demonstrating that more than one species is involved in the diffusion and reaction process that occurs at the crude oil-caustic interface. Sharma et al. [23] proposed that the lowering in interfacial tension is probably caused by two different components; one being an acid with a low molecular weight and other having a significantly higher molecular weight. Dunning et al. [24] positively correlated crude oil interfacial activity with the Ni-porphyrin complex associated with asphaltenes. Khulbe et al. [25] separated, in a conventional manner, Lloydminster crude oil into two main fractions, namely asphaltene and maltene components. The maltene constituents were then separated by column chromatography into five fractions, each of which was tested for its effect on interfacial tension against alkaline solutions. They found significant interfacial activity even with the maltene fractions and concluded that asphaltenes by themselves were not responsible for the interfacial activity associate with untreated heavy oil against caustic solutions. The global reactivity of a given crude oil is defined by its "acid number", which is the number of milligrams of potassium hydroxide required to neutralize the acid in one gram of the oil. The exact value of the acid number will usually depend on how the measurement is made. As a reactivity index, this acid number may not always correlate directly with interfacial activity. For example, Ramakrishnan and Wasan [26] observed that a crude oil with a low acid number may exhibit high interfacial activity against caustic solutions.

2.3 Use of Alkalis in Enhanced Oil Recovery

2.3.1 Caustic and IFT Reduction

The use of alkalis in waterflooding has been extensively investigated. Nutting [27] described the use of alkali salts such as sodium carbonate and sodium silicate, dismissing the use of strong bases such as sodium hydroxide because of their excessive reactivity with crude oil. Recently, Campbell [28,29] stated that sodium silicate, sodium hydroxide, sodium carbonate, and sodium phosphates are the mostly widely used reagents for alkaline water flooding. These reagents, in the majority of cases, are added to the flood water to improve the oil recovery. This can be achieved by the in-situ generation of surfactant soaps by the interaction of the alkali with the carboxylic acids present in the crude oil. It was observed that the formation of soap molecules is mainly responsible for the lowering of interfacial tension which is necessary for enhanced oil recovery. Cooke et al. [30] suggested that IFT values below 2.0 mN/m are required for additional oil to be recovered from a caustic flood. Several researchers stated the accumulation of the surface-active soap at the oil-water interface is time dependent, therefore the IFT becomes dynamic. This dynamic behavior fuelled the controversy among researchers concerning which IFT value would be operative in an alkaline flooding of an actual field situation. Some researchers argue that equilibrium IFT values are representative in the actual field, while others stated that the minimum IFT obtained in dynamic measuereents is

the most applicable value. McCaffery [31] believed that the minimum IFT would be unlikely for oil mobilization, since this ultra-low IFT is attained at a short time after the initial oil-caustic contact. Rubin and Radke [3] stated that the minimum IFT observed using the spinning drop tensiometer is indicative of the lowest achievable reservoir equilibrium value. Later, deZabala and Radke [32] confirmed Rubin and Radke's point of view. They obtained IFT data from multiple contacting of a fixed alkaline solution with fresh acidic oil and observed that the minima were close to those for the single contacts..

2.3.2 Mechanisms of Alkaline Oil Recovery

To elucidate the mechanisms postulated for enhanced oil recovery by caustic waterflooding, much work has since been done. Nutting [27] believed that alkaline solutions released residual oil from adherence to the reservoir rock matrix. He stated that caustic inhibited the formation of semi-solid, oil-water interfacial films. Atkinson [33] reported that caustic solutions had the ability to overcome the capillary forces, viscous resistances to flow, and adhesion of the oil to the sand, and release the oil. Subkow [34] reported that the formation of an oil-water emulsion in the pore spaces was an important step for improvement oil recovery. Apparently, the disparate behavior of alkaline flooding processes resides in the wide variation of alkali-oil and alkali-rock interactions. Recently, Johnson [35] outlined the various proposed mechanisms. These include :

1. Lowering of Interfacial Tension,
2. Emulsification and Entrainment,
3. Emulsification and Entrapment,
4. Wettability Reversal (oil-wet to water-wet),
5. Wettability Reversal (water-wet to oil-wet),
6. Emulsification and Coalescence.

In addition to interfacial tension reduction, wettability reversal and emulsion formation appeared to be the dominant concepts for all these proposed mechanisms.

Lowering of Interfacial Tension

In oil recovery processes, the capillary forces cause large quantities of oil to be left behind in well-swept zones of water flooded oil reservoirs. Capillary forces are the consequence of the interfacial tension between the oil and water phases and they resist externally applied viscous forces. Lowering of the interfacial tension recovers additional oil by reducing the capillary forces. Several processes have been tested in the laboratory as well as in the field, the predominant enhanced oil recovery techniques for achieving low interfacial tension being micellar and alkaline flooding. In such processes, the surfactants are adsorbed at the oil-water interfacial and can thus reduce the interfacial tension. To mobilize the residual oil, ultra-low to low interfacial tensions are required.

Wettability Reversal

It was shown by Owen and Archer [36] that increasing the degree of water wetness of the reservoir rock increases the ultimate oil recovery. The wettability was reported as decreasing the water-oil contact angle. Wagner and Leach [37] confirmed this hypothesis by using high-pH chemicals. Johnson [35] believed that the increased oil recovery is the result of two mechanisms: (i) a relative permeability effect, that causes the mobility ratio of a displacement to decrease, and (ii) a shifting of the capillary desaturation curve. Cooke et al. [30] have reported improved oil recovery with increased oil wetness. However, Ehrlich et al. [38] showed that oil recovery is a maximum when the wettability of a permeable medium is neither strongly water-wet nor strongly oil-wet. Therefore, the change in the wettability rather than the final wettability of the medium, appears to be the important factor. This change causes the trapped residual oil, originally discontinuous in the porous medium, to be converted to a continuous wetting phase. In addition to the low interfacial tension present, an emulsion of water droplets is formed and they become trapped in the porous medium. The resulting phase redistribution then makes both phases vulnerable to recovery through viscous forces.

Emulsion Formation

Alkaline chemicals can cause improved oil recovery through the formation of emulsions [39]. The in-situ emulsification of residual oil is a consequence of the reduction in interfacial tension. The emulsification produces additional oil in at least three ways: entrainment, entrapment and coalescence.

The in-situ emulsification of the crude oil, and entrainment into a continuous flowing caustic water, have been suggested by Subkow [34]. The caustic has the ability to prevent adherence of the oil to the sand surface. The condition necessary for continuous entrainment appears to be maintaining the interfacial tension at a low level while moving the mixture through the reservoir.

For the emulsification and entrapment mechanism, many studies have shown that the residual oil in a water-wet porous media could be emulsified and moved downstream, to be entrapped again by pore throats too small for the oil emulsion droplets to penetrate. This mechanism results in a reduced water mobility that improves both vertical and areal sweep efficiency. This mobility ratio improvement is particularly important in water flooding viscous oils where sweep efficiency is poor. The improvement in sweep efficiency, in this type of reservoir, caused by a more favorable mobility ratio would be more important economically than the recovery of residual oil left behind after a water flood. As proposed by Castor eltal. [40] the entrained oil droplets must coalesce to form a stable oil bank, depending on the stability of the in situ-emulsification.

2.4 Rationale for Aqueous Phase Viscosity Enhancement

2.4.1 Use of Polymers in Enhanced Oil Recovery

Caustic water flooding as an enhanced oil recovery process, has been very popular to increase oil recovery because caustic reagents are widely available and cheap. This process is applicable to moderate heavy oils. Indeed, it is inefficient when the reservoir contains high permeability streaks even in heavy oil reservoirs. Caustic reagents undertake severe losses due to adsorption and ion exchange with matrix minerals. Also in caustic waterflooding, the mobility control is unfavorable which results in an excessive fingering and stranding of oil ganglia. Incorporation of water-soluble polymeric materials has been successfully used for mobility control and thus lead to higher oil recovery efficiency. This typical enhanced oil recovery process is specially developed for application to reservoirs containing low to medium viscosity crudes. However, when mobility of water is equal to or lower than the mobility of oil, the efficiency of this process is optimized. Polymers, when added to caustic waterflood, reduce the mobility by two mechanisms. First they increase the water viscosity and second they interact with the reservoir rock. By reducing the mobility of water, the overall recovery efficiency is improved through displacement efficiency, areal sweep and vertical conformance. Recently, several researchers [41,42,43] investigated the possibility of improved chemical processes, including the incorporation of polymeric materials to micellar and alkaline flooding

to improve oil recovery. Potts and Kuehne [42] obtained higher oil recovery when alkaline and polymer are injected in a single slug and move together through the reservoir. Latter, Shuler et al. [43] found that a combination process, referred to micellar/alkaline/polymer, recovered more than 80 % of the waterflood residual oil in comparison to micellar/polymer and alkaline/polymer processes.

2.4.2 The Polymers

Several polymers have been considered for enhanced oil recovery, Xauthan gum, hydrolyzed polyacrylamide, polyacrylamide, copolymers of acrylic acid and acrylamide, polyethylene oxide and polyvinyl alcohol. They are very soluble in water and they may show complex behavior when injected to oil reservoirs. All the commercially attractive polymers fall into two classes, polyacrylamide and polysaccharide. Polyacrylamides, as used in waterflooding have undergone partial hydrolysis, which causes anionic carboxyl groups ($-COO^-$) to be scattered along the chain. This anionic character accounts for many of its physical properties. The degree of hydrolysis has been selected to optimize certain properties such as water solubility, viscosity and retention [44].

In practice, the choice of a polymer is usually restricted by the extent to which it is degraded by heat and salinity associated with the reservoir. Its reactivity controls the resistivity factor and polymer losses due adsorption on reservoir matrix rock. Generally, the molecular weight, the size, the shape factor and the chemical

nature of the side groups controls the solution viscosity. The stability of this polymers depends on the chemical configuration of the molecules and on the chemical and physical conditions to which they are subjected. From experimental point of view, it is necessary to determine several basic properties in order to decide on the best polymer and its most effective concentration. Screening tests includes the phase behavior, interfacial activity, dispersion and viscosity.

2.4.3 Polymer Properties

Viscosity Relation

The most important physical property of a polymer is the viscosity of its aqueous solution. Polymer solutions are characterized by their viscosity–concentration relationship. This relation has been traditionally modeled by Flory-Huggins equation [45] :

$$\mu = \mu_1[1 + a_1 C_p + a_2 C_p^2 + a_3 C_p^3 + \cdots +] \tag{2.1}$$

where C_p is the polymer concentration in the aqueous phase, μ_1 is the solvent viscosity and a_i's are constants. The linear term in Eq. 2.1 accounts for the dilute range. In practice polymer are usually used as thickener for aqueous solution. A more fundamental way of measuring the thickening power of a polymer is through its intrinsic viscosity, defined as the a_1 term in Eq. 2.1 [45]. The intrinsic viscosity, $[\mu]$, for any given polymer-solvent pair, increases as the molecular weight, M, of the

polymer increases according to the following equation, known as Mark-Houwink equation :

$$[\mu] = K'M^a \tag{2.2}$$

The exponent, a, varies between about 0.5 and 1.5 and is higher for good solvents such as fresh water. Ployacrylamide in water has K' (Mark-Houwink constant) value of 68×10^{-5} and a of 0.66 at 30°C [46].

Non-Newtonian Behavior

Many polymer solutions exhibit a non-Newtonian character, with increasing shear rates ($\dot{\gamma}$) causing larger decrease in measured viscosities. The typical behavior of polymer solutions is pseudoplastic mode which can be approximated by the power-law [46].

$$\mu = m\dot{\gamma}^{n-1} \tag{2.3}$$

It is also known as shear thinning where m and n are the power-law coefficient and exponent, respectively. For shear thinning fluids, $0 < n < 1$; for Newtonian fluids, n=1 and m becomes the viscosity. The shear thinning behavior of the polymer solution is caused by the uncoiling and unsnagging of the polymer chains when they are elongated in shear flow. Consequently, the resistance to flow (i.e. viscosity) becomes smaller as the rate of shearing increases. The power-law model (Eq. 2.3) describes fairly well the behavior of polymer solutions except in the region of low shear rates where it gives an infinite measured viscosity.

Effects of Alkaline and Brine

Viscosity of polymer solutions is very sensitive to alkalinity and more profound to salinity. It decreases as the salt concentration increases. The synergistic effect of combining polymer with alkaline and salt has been studied else where [47]. Mungan et al. [48] have reported that electrolyte tend to suppress the pseudo-plasticity of polymer solutions. Therefore, he observed that salt has the effect of neutralizing the intrinsic electrical charges on the polymer molecules. This causes the polymer to behave non-ionized. Therefore the polymer chains coil up which results in a decrease in the interactions between the polymer particules. These effects cause the solution viscositv and its dependence on the shear rate to decrease. The synergistic effect is more pronounced in presence of divalent cations [48]. Ryles [49] studied the thermal stability of polyacrylamide in alkaline solution. He observed that polyacrylamide stability is independent of the alkaline reagent and molecular weight, but is limited by thermal degradation to temperature less than 120°C. The degradation is determined by the rate of hydrolysis of amide groups which is found [49] to be very slow at 50°C and less.

2.5 Interaction of Caustic with Acidic Oils

The study of the interaction of caustic reagents with acidic oils has been extensively investigated [3,26,31,50–56]. There have been several studies on both equilibrium

and dynamic interfacial tension of such systems. From equilibrium consideration, the following interfacial reactions were used by almost all the researchers to model this oil-caustic interaction.

2.5.1 System Chemistry

As reported in previous studies, the mixture of acidic species in the crude that react with the caustic can be conveniently represented by a single species, HX. This acid distributes itself between the oleic phase and the aqueous phase in constant distribution ratio, according to the equilibrium relationship;

$$HX_o \rightleftharpoons HX_w \tag{2.4}$$

and

$$K_D = \frac{C_{HX_o}}{C_{HX_w}} \tag{2.5}$$

where HX_o is the oleic-phase acid, HX_w is the aqueous phase acid and C_i is the concentration of species i at equilibrium. The distribution ratio, K_D should be very large due to the extremely low concentration of acid in the aqueous phase under normal conditions.

In the aqueous phase, the acid dissociates to its ionic form (surface-active species X^-) and hydronium ions. The dissociation equilibrium is governed by the aqueous phase pH and is represented as :

$$HX_w \rightleftharpoons H^+ + X^- \tag{2.6}$$

and

$$K_X = \frac{C_{H+} C_{X-}}{C_{HX_w}} \tag{2.7}$$

where K_X is the dissociation constant of HX. The equilibrium ionic concentrations are influenced by the dissociation constant for water:

$$K_w = C_{H+} C_{OH-} \tag{2.8}$$

At high caustic concentrations, a surface-inactive soap complex NaX is formed at the aqueous side of the interface [26]. This salt was presumed to be oil soluble due to the hydrophilic nature of the hydrocarbon chain of X and its dissociates almost completely in the aqueous phase to produce sodium ions and the surface-active species X^-. According to Ramakrishnan and Wasan [26], and later by Borwanker and Wasan [54,55], the formation of NaX and its partitioning is represented by:

$$Na^+ + X^- \rightleftharpoons NaX_w \tag{2.9}$$

with an association equilibrium constant defined as

$$K_{s1} = \frac{C_{Na+} C_{X-}}{C_{NaX_w}} \tag{2.10}$$

and

$$NaX_w \rightleftharpoons NaX_o \tag{2.11}$$

with a distribution ratio:

$$K_{s2} = \frac{C_{NaX_w}}{C_{NaX_o}} \tag{2.12}$$

By combining Eqs.(2.7) and (2.9) the global equilibrium parameter governing the formation of NaX and its partitioning, is as follows:

$$K_s = K_{s1}K_{s2} = \frac{C_{Na^+}C_{X^-}}{C_{NaX_o}} \tag{2.13}$$

The system chemistry used here is summarized in Fig. 2.1.

2.5.2 Interfacial Resistance and Dynamic IFT Minimum

The transfer of surface-active species across a liquid-liquid interface has been studied by England and Berg [2]. Their analytical solution for the transfer of surfactant takes into account the effects of molecular diffusion in both bulk phases, the adsorptive accumulation at the interface, and energies of adsorption and/or desorption. Dealing with non-reacting systems, their analysis showed that interfacial resistances signified by sorptive barriers were largely responsible for the phenomena of dynamic IFT. As demonstrated by Sherwood and Wei [1], the Fickian diffusion model adopted by England and Berg is inadequate because the problem is essentially a convective diffusion. The convective diffusion has been used whenever convection currents were involved. In a reacting system, interfacial turbulence is generated by the gradient in chemical potential. This phenomenon is known as Marangoni disturbances or interfacial tension-driven interfacial disturbances [57,58]. In consequence, convective diffusion in the immediate vicinity of the interface was spontaneously set up. Sternling and Scriven [59] outlined clearly the conditions where interfacial turbulence was more intense. These include:

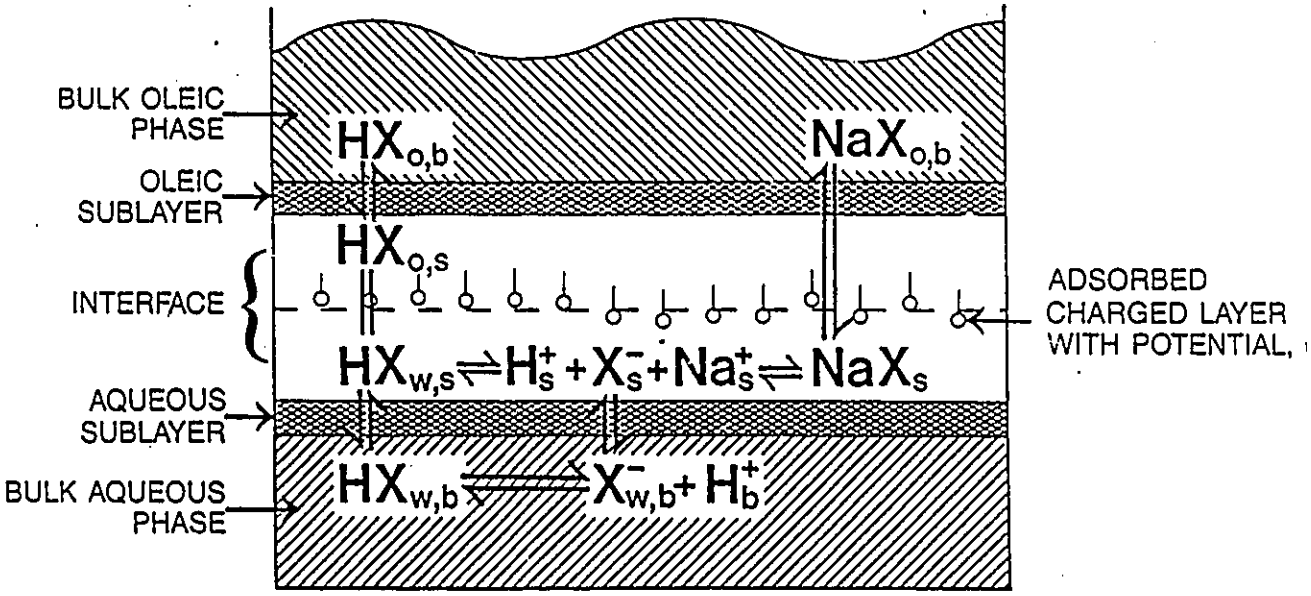

Figure 2.1: A Geometrical Model of the Interface

1. where solute was being transferred out of the phase of higher viscosity,
2. where solute was being transferred out of the phase of low diffusivity,
3. where there were large differences in kinematic viscosity and solute diffusivity between the two phases,
4. where steep concentration gradients were present near the interface,
5. where IFT was highly sensitive to the concentration of solute,
6. where both phases had low diffusivities and viscosities,
7. where there were no surface-active species present,
8. where the interfaces were of large extent.

Rubin and Radke [3] extended the analysis of England and Berg [2] to the case of phases of finite extent using Nernstian theory to model convective diffusion. Their experimental data obtained by spinning drop tensiometry did not allow any quantification of sorption kinetic parameters because the interfacial area was not conserved and because of hydrodynamic end effects in the spinning capillaries. Later Brown and Radke [60] allowed for areal variations of the oil droplet spinning in the capillary tube of the spinning drop tensiometer. Their theoretical and experimental analysis showed that dynamic tension minima for acid oils in contact with alkali are caused by significant sorption barriers at the oil-water interface. It is well accepted now that the acid in the crude oil, upon contacting with alkali solutions, transport

out of the oil and react to produce surface-active salts which dramatically reduce the IFT to low levels. The reduction in IFT is followed thereafter by a slow rise to a high level. Rubin and Radke [3] postulated that the transfer of the surface-active species from the oil to the aqueous phase may be conceptualized in five steps : (1) convective-diffusion from the oil phase to the interface, (2) adsorption at the interface, (3) reaction at the interface, (4) desorption from the interface, and (5) convective-diffusion into the aqueous phase. The rates of these sequential events then determine the dynamic nature of the interfacial tension. deZabala and Radke [61] and deZabala [62] thought that, since the hydrolysis reaction is ionic in nature, it occurs instantaneously and the remaining four steps determine the kinetics of the overall process.

Bansal et al. [63] established from their investigation of electrophoretic mobility (i.e. charge density) and IFT measurement of crude oil-caustic systems, that the minimum in IFT corresponds to the maximum electrophoretic mobility. Later Rubin and Radke [3] and recently Sharma et al. [23] stated that the IFT minimum must occur concurrently with a maximum in surface-active species adsorption in order to properly satisfy the Gibbs adsorption equation. Therefore, the origin of dynamic tension minima is a result of the net accumulation of surface-active species at the interface. This tension minimum should be observed when either the net rate of adsorption is significantly higher than the net rate of desorption, or when the convective-diffusion resistance of the aqueous phase exceeds that of the oil phase.

Chapter 3

Experimental Aspects

3.1 Experimental Design

3.1.1 Selection of the Working Systems

Based on previous works [10,56], light paraffin oil was selected as the solvent in preparing the oleic phase systems. Linoleic acid was found to be more compatible with the paraffin oil over a wide concentration range. Consequently, this acid was used as the working reactant in the oleic phase. For the aqueous phase formulations sodium hydroxide was used as the alkaline reagent. A wide range of NaOH concentrations was used up to a maximum of 250 mM. Since polyacrylamide is a commonly used polymer in chemical enhanced oil recovery, we therefore decided to investigate this polymer in admixture with the caustic solutions. Another water-soluble polymer was also studied, namely polyvinyl alcohol.

3.1.2 Experimental Strategies

The working system selected in the preceding subsection is expected to exhibit dynamic interfacial tension behavior within a reasonable and measurable time period. In addition it is desirable to determine, a priory, the dynamic interfacial tension trends of caustic solutions (without polymer) in contact with the acidified paraffin oil. Having characterized the polymer-free alkaline solutions by interfacial tension, viscosity, density and pH measurements, known amounts of the polymer would then be introduced. The interfacial behavior of this composite aqueous phase contacted with the acidified paraffin oil would then be determined. In order to completely characterize the caustic-polymer formulation, viscosity, density, pH and phase stability studies would then be conducted. The strategies which were developed, and their various steps, are as follows:

Strategy 1: Selecting working acid concentrations:

step1: Prepare various linoleic acid concentrations up to 100 mM in paraffin oil.

step2: Perform dynamic IFT measurements with distilled water and various NaOH solutions.

step3: Determine acid concentrations which produce the greatest interfacial activity.

step4: Measure physical properties such as density and viscosity.

Strategy 2: Dynamic IFT study for polymer-free NaOH solutions:

step1: Fix the acid concentration at the optimum as determined from Strategy 1.

step2: Prepare various NaOH solutions in distilled, deionized water.

step3: Perform dynamic IFT measurements with the NaOH solutions and the selected acid concentration.

step4: Measure density, pH and viscosity of the NaOH solutions.

Strategy 3: Dynamic IFT studies for reference polymer solutions:

step1: Screen various polymers for solubility and phase compatibility in NaOH solutions.

step2: Select working polymer concentrations from results of step1.

step3: Prepare blank polymer solutions (without NaOH).

step4: Measure dynamic IFT of the polymer solutions with the fixed acid concentration.

step5: Determine pH, viscosity and density of the polymer solutions.

Strategy 4: Dynamic IFT studies for polymer-caustic systems:

step1: Select working caustic and polymer concentrations from previous strategies.

step2: Prepare polymer-caustic solutions.

step3: Measure dynamic IFT of the polymer-caustic solutions with the fixed acid concentration.

step4: Determine pH, viscosity and density of the polymer-caustic solutions.

Table 1 gives the exact specifications of the reagents used in this study.

Table 1: Specifications of Reagents

NAME	SPECIFICATION	REMARKS
Sodium Hydroxide	Fisher Certified,ACS,Pellets	used as supplied
Polystyrene	BDH, Pellets M.W. 2-300,000	used as supplied
Polyvinyl alcohol	BDH, Granular M.W. 115,000	used as supplied
Polyacrylamide (non-ionic)	SP[2], Granular Nominal M.W. 5-6,000,000	used as supplied
Toluene	Fisher Certified,ACS	used as supplied
Linoleic Acid	Fisher Reagent,Purified	used as supplied
Light Paraffin Oil	BDH	used as supplied
Heavy Paraffin Oil	BDH	used as supplied
Water	Double distilled and deionized	

3.2 Measurement Procedures

3.2.1 Preparation of Working Solutions

Double distilled, deionized and deaerated water was used in preparing all aqueous solutions. In most cases, a stock caustic solution of 500 mM NaOH was freshly prepared, from which diluents were made to obtain the required concentrations. Stock polymer solutions of 5 % wt polyvinyl alcohol and 0.5 % wt polyacrylamide were freshly prepared and then used to formulate the various polymer solutions used for the different experiments. The different polymeric materials were added to the caustic solutions in amounts calculated to achieve a predetermined viscosity enhancement. A stock solution of 100 mM linoleic acid in paraffin oil was used to prepare the acidified oleic phases.

3.2.2 Pre-run Trials

Preliminary tests were performed in order to select appropriate operating speeds and oil droplet volumes for the dynamic IFT measurements. In order to overcome buoyancy effects the capillary assembly of the spinning drop tensiometer Model 500 was rotated at speeds ranging from 7500 rpm to 9000 rpm [64]. Various oil droplet volumes were used to conduct the IFT studies. For the majority of the systems covered in this study, the most appropriate droplet volumes were in the range of 2–3 μl. Screening tests were also conducted with various polymers for solubility

and phase compatibility in caustic solutions.

The appropriate cleaning procedure for all containers, glassware, needles and syringes that came into contact with the experimental solutions (either aqueous or oleic phases) was selected. This procedure consisted of an initial washing with water, followed by ethanol and then acetone. A further cleaning of all glassware was also made using hot chromic acid followed by water.

3.2.3 Low Dynamic IFT Measurement

Low IFT measurements were performed using the University of Texas Model 500 Spinning Drop Tensiometer (SDT). This apparatus is the most popular and convenient means of measuring low dynamic IFT. Apart from the buoyancy effects noted earlier [64], IFT measurements using this technique are affected also by circulatory flows [65] as well as by imprecise temperature control [66]. However, recent studies [66,67] have confirmed that the method is fairly accurate and reliable for low IFT measurements.

Details of the general measurement procedure have been outlined by Gardner and Hayes [68]. For dynamic tension measurements, Reive [69] has describe in detail the procedure for loading the capillary assembly. Briefly, the procedure which was used in this study consisted of introducing a small droplet of oil into a glass capillary tube, approximately 2 mm in diameter and 100 mm in length, which had been previously filled with the aqueous solution. A Hamilton micro-syringe was

used for the injection of the oil droplet. The tube was then quickly inserted into the cap assembly and screwed into the rotating sleeve of the SDT. When spun, the droplet elongates due to rotational forces until a balance is struck between these forces and the interfacial forces.

All measurements were made at 25°C using an air cooling system. This system consisted of a refrigerated bath which served to control the temperature of the cooling air circulating in the capillary tube housing. The bath was set to control the temperature at 25°C by varying the rate of air circulation. The first reading was taken during the first minute of spinning time (within 30 seconds with practice), and subsequent readings were made at pre-determined intervals. At each time interval, the speed of rotation and the temperature of the housing capillary tube were recorded. All measurements were carried out in replicate for better precision.

3.2.4 Moderate Dynamic IFT Measurement

From a purely experimental point of view, the classical spinning drop tensiometer has a number of drawbacks which make the instrument less convenient for dynamic tension measurement. The University of Texas tensiometer is designed for air cooling of the rotor housing which makes a temperature control difficult to realize, especially when operating at high speeds and extended times. In fact, heat is usually generated in the motor and bearings, and this in turn heats up the capillary tube housing. This temperature gradient within the spinning capillary tube can

produce undesirable circulatory flows [65]. Also, the interfacial age determination is quite imprecise, because measurement of the linear dimensions of the oil droplet are made during the course of the experiments. It is quite difficult and unreliable to make any measurement for constant time less than one minute. Often, drifting of the spinning droplet towards one end occurs, which makes dimension measurement difficult to achieve, especially when the droplet length has to be measured simultaneously.

For more accurate and precise dynamic IFT measurements in the low and moderate tension regimes, Chiwetelu et al. [70] have successfully modified the basic configuration of the University of Texas tensiometer. A schematic diagram of the modified SDT is shown in Fig. 3.1. The modification consists essentially of integrating the microphotography into the classic SDT and is detailed in the following subsections.

Elements of the Measurement System

This new technique eliminates the need for in-situ linear measurement. Therefore, a more precise and reliable measurement of the droplet dimensions can be made, and it gives a better correlation of the experimental data with the age of the interface. Additionally, the images of the experimental droplet at any desired time intervals are held permanently on photographic negatives. Drifting oil droplets do not pose

any further problems to the experimentalists and the necessity for simultaneous measurement of the length and width of the spinning droplet no longer arises. A temperature control system for the measurement chamber has also been added to the modified tensiometer. The major hardware of the so-called spinning drop photo-tensiometer consists of the following :

1. The University of Texas SDT model 300 instrument excluding the stroboscope and the microscope accessories.

2. A high power and variable voltage tungsten lamp that was substituted for the stroboscope, as can be see in Fig.3.1. This was necessary in order to ensure adequate illumination for high speed micro-photography. A green filter and a heat shield were installed in front of the tungsten lamp in order to prevent excessive radiant heat reaching the measurement chamber.

3. An optical system that includes a substitute microscope equipped with a flat eye piece and a camera assembly. The camera assembly itself is an Olympus Model PM-10-M system consisting of a manual-exposure body fitting loosely into the microscope unit. The exposure body itself carries a focusing telescope and a 35 mm camera back.

4. A refrigerated Haake F3 bath set to control at a temperature which enables the measurement chamber to be kept at $25 \pm 0.1°$ C.

5. A Gralab Model 625 digital timer/intervalometer used for precise monitoring of the duration of the experiment and also for determining the frequency for taking the photographic shots.

6. A Scherr-Tumico optical comparator Model 20-4200 equipped with direct digital horizontal and vertical scales by means of which the linear dimensions of the rotating droplet could be obtained from photographic negatives.

Optical System Assemblage and Calibration

Prior to actual tension measurement, the tungsten lamp had to be calibrated in order to have a sufficient background illumination at the image plane of the camera system. For this purpose, an exposure meter was used to select an appropriate voltage for the lamp. The optical system assemblage consisted of aligning the microscope and the camera assembly perfectly on the same optical axis as the incident light from the tungsten lamp passing through the mid point of the access windows of the capillary tube housing. Next, the flat-field eye piece was inserted into the slot provided for it on the microscope. Finally, the high resolution film (Kodak TP 135-36) was loaded into the camera back after ensuring that all necessary optical adjustments had been made.

Calibration of the optical system was done using an accurately machined stainless steel rod. The rod surface was uniformly coated with a thin film of black paint

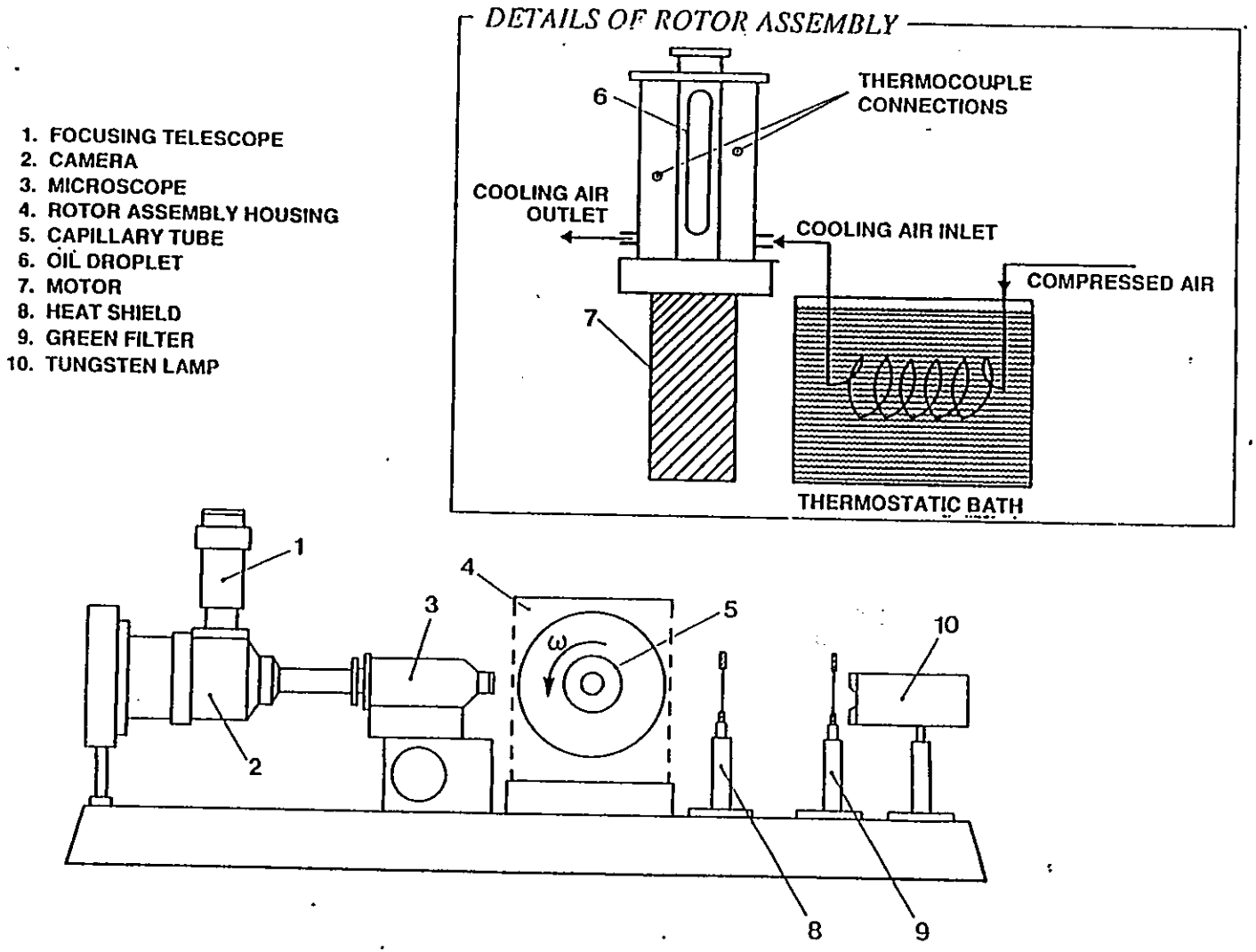

Figure 3.1: Schematics of the Modified Spinning Drop Tensiometer

in order to reduce reflectance and thus ensure that a sharply defined image of the rod was obtained. The capillary tube was first filled with distilled water and the rod carefully placed inside the tube. The loaded tube was slotted into the capillary tube housing of the rotor assembly and then spun at speeds of about 7000 rpm. Thereafter, the rod was aligned on the optical axis, focused with the aid of the focusing knob of the microscope, and then photographed. The measurements of the linear dimensions of the rod's images were made from photographic negatives. A comparison of the dimension of the magnified image with the actual size of the rod yielded magnification factors for both length and width measurements provided that the optical system remained unchanged whenever an oil droplet was substituted for the rod.

IFT Measurement Procedure

The apparatus was set as previously described. The measurement procedure including preliminary runs, loading of the capillary tube and temperature control, was the same as outlined for the classic SDT. Thus, photographs of the spinning droplet were taken at predetermined intervals in response to audio signals received from the intervalometer. At each time interval, the speeds of rotation and the temperature of the measurement chamber were recorded.

Measurement of Linear Dimensions of Droplet

After film processing and development, measurements of the linear dimensions of the droplet's image were made from photographic negatives using the optical comparator. Each frame to be measured had to be laid flat on specially made frame holders [56]. The mounted frame was then fixed on the vice of the comparator and the image of the droplet properly focused on the measuring screen. The vertical and horizontal axes of symmetry were located with the aid of the vertical and horizontal scales of the instrument respectively. Moving along the axes, the maximum length and maximum width of the image were registered.

3.2.5 IFT Calculation

The basic principle governing the design of the spinning drop tensiometer (SDT) is the balance, at gyro-static equilibrium, between capillary and centrifugal forces acting on the rotating drop :

$$\Delta P = \gamma\left(\frac{1}{R_1}+\frac{1}{R_2}\right) = \frac{2\gamma}{R_o} - \frac{\Delta\rho\omega^2 y^2}{2}$$

The IFT's are calculated using various schemes, which included the following:

(i) For drops approaching infinite length, i.e., L>4D, Vonnegut's solution [9] is applicable and this is given by:

$$\gamma = \frac{\Delta\rho\omega^2 y_o^3}{4} \tag{3.1}$$

Taking into consideration the refractive index of the aqueous phase (generally water), Reive [69] modified Eq. 3.1 as follows:

$$\gamma = 0.522 \times \frac{\Delta\rho d^{*3}}{T^2} \tag{3.2}$$

(ii) For finite drops (i.e. L < 4D), Slattery and Chen [71] have presented an analysis for the spinning drop, by which the interfacial tension and drop volume can be calculated for all drop shapes from the measured maximum drop diameter and drop length. The expression for the interfacial tension and drop volume given by Slattery and Chen, after introduction of the refractive index correction, are :

$$\gamma = \frac{1}{2}\left(\frac{d^*}{2r^*_{max}}\right)^3 \frac{\Delta\rho\omega^2}{1.33^3} \tag{3.3}$$

(iii) In order to extend its limited applicability, Princen et al. [8] extended Vonnegut's approximate solution using a numerical solution based on exact equations. Using this solution, IFT from SDT data for finite and semi-finite drops can be calculated from the linear dimensions when the drop volume, speed of rotation and density difference between the two phases are known.

Ring Tensiometry

The initial IFT values cannot be measured by means of the SDT. Therefore classical tensiometry is used. This method involves the determination of the force to detach

a platinum ring from the interface between two fluids. It is generally attributed to du Nouy [4]. By equating the vertical pull, f, on the ring at the moment that the ring breaks away from the surface, to the radius R of the ring, the apparent tension value can be calculated as follows:

$$\gamma_{ap} = \frac{f}{4\pi R} \tag{3.4}$$

However, since the surface tension force does not in general act exactly vertically, a correction factor F is necessary in Eq. 3.4 [4]:

$$\gamma_t = \gamma_{ap} \times F \tag{3.5}$$

where :

$$F = \left(\frac{\gamma_t}{\gamma_{ap}}\right) = \text{function}\left(\frac{R^3}{V}, \frac{R}{r}\right) \tag{3.6}$$

The correction factor F can be determined using the tables established by Harkins and Jordan [72].

3.2.6 Density, pH and Viscosity Measurement

Density Measurement

The densities of all working solutions were measured using the Anton Parr Precision densitometer model DMA O2C. The temperature of this unit was controlled to 25 ° ± 0.01° C by means of a Techneurop programmable temperature controller in series with a Neslab RTE-4 Endocal refrigerated circulating bath. The density

was calculated using a software package run on a commodore PET model 4032 microcomputer which converts the periods indicated on the Anton Parr densitometer directly to densities using high purity water as the reference liquid according to the equation:

$$\rho_1 - \rho_2 = K_{ap}\left[T_1^2 - T_2^2\right] \tag{3.7}$$

pH Measurement

The pH of the aqueous solutions was measured with the Orion Research digital ionalyzer model 501 using Fisher Scientific's high pH glass electrode. Calibration of the pH meter was carried out using pH 4 and pH 7 buffers prior to each measurement. Room temperature of 23 to 25° C prevailed during most of the measurements.

Viscosity Measurement

Pre-calibrated Cannon-Fenske viscometer was used for both the oleic phase and alkaline solutions, and an oil bath was used for temperature control. For polymer solutions, viscosity measurements were made after 15 minutes equilibration in a 25° C bath using the UL Adaptor arrangement of the Brookfield Synchro-lectric viscometer. The adaptor, consisting of a precision cylindrical spindle inside a stainless steel tube, allowed the measurement of viscosities in the range of 1 to 100 mPa.s with 2 % reproducibility.

Chapter 4

Results and Discussion

4.1 Physical Properties of Working Systems

4.1.1 Properties of the Aqueous Solutions

The physical properties required in this study (such as density, viscosity, and pH) were measured for all of the aqueous solutions. Tables A1 and A2 of Appendix A list the density values for the solutions at different polymer (polyvinyl alcohol (PVA) and polyacrylamide (PAM) respectively) and NaOH concentrations. The density of distilled water in Tables A1 and A2 measured at 25°C was 997.0461 kg/m^3. As the concentration of PVA in neutral water was increased progressively the density of the resulting solutions also increased marginally, with only about 0.7 % increase (over that of water) in the density of the maximum PVA concentration of 3.0 % by weight. A similar trend in the densities of the caustic solutions containing varying amounts of polymer is also evident from the data presented in Tables A1 and A2.

The density of 250 mM caustic solution was 1007.6526 kg/m^3, while the addition of 3.0 % by weight PVA increased the density by only 0.6 %.

The pH values for the working aqueous solutions are listed in Tables A3 and A4. As expected, the higher the concentration of NaOH in neutral water, the higher the pH value. In Table A3, we find that starting with neutral water at a pH of 7.03, the addition of PVA up to 3.0 % by weight decreased the pH of the resulting solution marginally to about 6.6. There is no significant variation in pH with an increase in PVA concentration. For PAM, a similar trend can be seen in Table A4 except that these polymer solutions have a slightly higher average pH value (6.9). For these two polymers, the pH value of their solutions in neutral water is typically in the range of 5-7 [73]. In Tables A3 and A4, we find also that for each working NaOH concentration, the addition of polymer to the caustic always resulted in a slight reduction in pH. One probable explanation for this reduction in pH following the introduction of polymer is loss of caustic from enhanced hydrolysis of the carboxylic group in the polymer chain.

Data for the viscosities of the various polymer, caustic and polymer-caustic solutions employed in this study have been tabulated as shown in Tables A5 to A8. Those results were obtained by using a Brookfield Synchrolectric viscometer at different shear rates. Generally, the viscosity of caustic solutions (without polymer) was about 1.0 mPa.s independent of NaOH concentration. In the case of polymer solutions (without caustic) in water, we find a dramatic increase in solu-

tion viscosity with increasing polymer concentration. For example in Table A5, the addition of 1.5 % by weight of PVA increased the viscosity of the aqueous phase to 6.2 mPa.s. Further increase in PVA concentration to 3.0 % by weight resulted in a solution whose viscosity was found to be 28.0 mPa.s. A similar trend was also obtained with PAM as can be seen from Table A6. Because this is a high molecular weight polymer, the viscosity of a 0.3 % by weight solution in water was as high as 21.1 mPa.s. Polymer solutions in water generally exhibit non-Newtonian behavior, which may be classified as pseudo-plastic or dilatant [46]. In view of this characteristic, we carried out additional viscosity measurements at various shear rates as indicated in Tables A7 and A8. In Table A7, the viscosity of 0.6 % by weight PVA in water at 6 and 12 rpm was found to be 2.60 and 2.50 mPa.s respectively. However, at higher rotational speeds, the viscosity decreased substantially (1.90 mPa.s at 30 rpm, 1.10 mPa.s at 60 rpm). For 3.0 % by weight PVA solution, viscosity measurement with the Brookfield instrument could be obtained only at speeds of 6 and 12 rpm respectively. Solutions of PAM in water also exhibited this pseudo-plastic behavior similar to that shown by PVA. The drop in viscosity at higher shear rates is quite evident for the two polymers. When various amounts of polymer are added to caustic solutions (see Tables A5 and A6), the viscosity of the polymer-caustic mixture increased considerably. In Table A6 with PAM as the working polymer and caustic concentration of 250 mM, the presence of 0.30 % by weight of the polymer increased the solution viscosity from 1.00 to 19.35 mPa.s. Here also, the polymer-caustic solutions exhibited pseudo-plastic behavior

the details of which are presented in Tables A7 and A8. As was observed earlier for caustic-free polymer solutions, those polymer-caustic mixtures also showed a significant drop in viscosity at higher shear rates. This reduction in viscosity can be attributed to shear degradation of the polymer at increasingly high shear rates.

4.1.2 Physical Properties of the Oleic Solutions

Table A9 contains density and viscosity data for the various oleic solutions employed in the study. The crude oil used in this work, namely Lloydminster crude from Saskatchewan (well A2-12-49-W3) has a density of 970.5 kg/m^3 at 25°C. Other properties which have been determined earlier [69] include API gravity of 14.3 and in-situ viscosity of 3500 mPa.s. A 10 % by volume solution of this crude in toluene had a density of only 858.0 kg/m^3 and a viscosity of 1 mPa.s. By adding increasing amounts of polystyrene up to 10 % by weight the density of the composite solution increased substantially as can be seen in Table A9. The viscosity of the polystyrene-Lloydminster-toluene formulations also increased with the addition of amounts of polystyrene but the effect was more manifest at polymer concentration above 5 % by weight. When the crude oil was replaced by 10 mM linoleic acid, Table A9 shows that the density was relatively unchanged and the solution viscosity was only slightly lower than the value measured for the crude oil-polystyrene system. For the simulated oleic phase light paraffin oil was used as the base solvent. This oil has a density of 838.8 kg/m^3 and a viscosity of 19.260 mPa.s. The addition of increasing

quantities of linoleic acid to the paraffin oil did not change the density appreciably, but the viscosity increased marginally at higher acid concentrations.

4.2 Transient IFT Behavior of Oil/Caustic Interfaces

4.2.1 Effect of Acid Content of the Oleic Phase

The effects of oil acidity on transient IFT were experimentally measured for systems in which linoleic acid at different concentrations was dissolved in light paraffin oil. For comparison purposes the IFT behavior of a reacting system was determined for Lloydminster crude oil of acid number of 0.9 (mg KOH/g oil) [69] in contact with an aqueous 25 mM NaOH solution. The experimental data are displayed in Fig. 4.1 and are typical of most crude oil/ alkaline systems [23,25,74]. In this figure, as well as those of Figs 4.2 and 4.3, replicate experimental data for each system were plotted in order to show the degree of precision of the measured values, and a cubic spline fit of the experimental points was used. Upon contacting the acid with caustic, the IFT drops sharply on account of the initial formation of surfactant by reaction at the droplet surface. Shortly thereafter, the IFT reaches its minimum and increases steadily as the acid in the oil is gradually depleted by reaction.

The effect of varying acidity of the oleic phase on dynamic IFT was investigated by using a system consisting of a dilute solution of linoleic acid dissolved in paraffin

oil. The transient IFT behavior of this system in contact with 25 mM NaOH solution is depicted in Fig. 4.2.

It is evident that this oleic phase exhibited dynamic IFT trends similar to those found using Lloydminster crude oil, but with higher absolute IFT values. From Fig. 4.3, it is seen that the relative rates of IFT decrease and increase, and the IFT minimum and its corresponding time, depend to a great extent on the acid content of the oil phase. However, for 1 mM linoleic acid solution (Fig. 4.2(a)) the IFT obtained after 50 seconds of spinning was 0.53 mN/m. The tension decreased to a minimum of 0.26 mN/m at 800 seconds, and then increased to approach an equilibrium value of 0.36 mN/m. As can be seen in Fig. 4.2.(b), the IFT for 10 mM linoleic acid reached its minimum of 0.20 mN/m at a later contact time of 1000 seconds. At higher acid concentrations, lower IFT minima were obtained, and the minima occurred at correspondingly longer times. As can be seen, at concentrations greater than 20 mM the rates of increase in IFT after attaining the minimum were reduced. For 100 mM linoleic acid (Fig. 4.2(d)), the IFT reached its minimum of 0.14 mN/m at 1500 seconds and attained thereafter an equilibrium value of 0.16 mN/m. From this set of experiments, it is observed that for a single acid present in the oleic phase, the higher its concentration is, the greater is its interfacial activity. With crude oils, several researchers [26,39] have found no direct relationship between acid number of crude oil and its interfacial activity. Depending on the applicable caustic concentration, oils with low acid number have produced

lower IFT values than other oils with higher acid numbers.

4.2.2 Effect of Varying Alkaline Concentrations

As previously mentioned, the system of linoleic acid dissolved in paraffin oil is characterized by an interfacial activity that increases with the acid concentration up to 100 mM. In enhanced oil recovery operations, typical acidic crude oils have an acid number ranging from 0.2 to about 3 (mg KOH/g oil). Therefore, it was decided that 10 mM linoleic acid concentration (corresponding to an acid number of 0.56) would be the working acid strength for all of the remaining sets of experiments. Accordingly, IFT data for this system in contact with a spectrum of NaOH solutions up to 500 mM were measured. These IFT data have been plotted as a function of the interfacial age in Figs. 4.5 and 4.6. The interfacial tension of paraffin oil against distilled water, as measured by the Du Nouy Ring tensiometer at 25°C was 50.10 mN/m, while for acidified paraffin oil the IFT value was only 36.2 mN/m. The decrease in IFT can be attributed to the interfacial activity of the carboxylic acid. Fig. 4.4 shows the dynamic IFT behavior when 10 mM linoleic acid (in paraffin oil) was contacted with double distilled water.

The IFT dropped gradually with spinning time from an initial value of 31 mN/m to an equilibrium value of 22 mN/m after 30 minutes. This significant interfacial activity exhibited by linoleic acid in contact with double distilled water indicates that the acid behaves like a weak surfactant in neutral aqueous media.

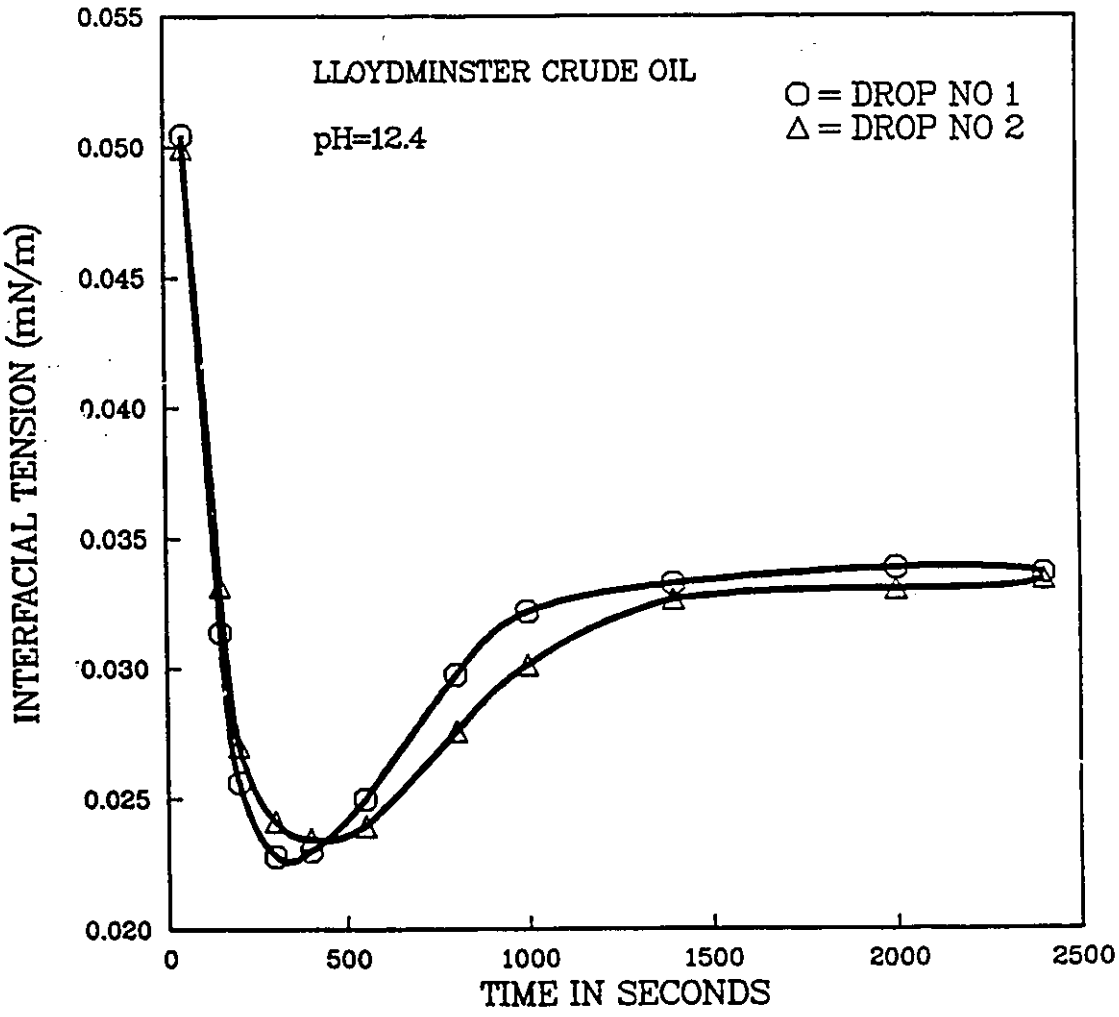

Figure 4.1: Transient Interfacial Tension behavior of heavy Lloydminster Crude Oil against 25 mM NaOH solution at 25° C.

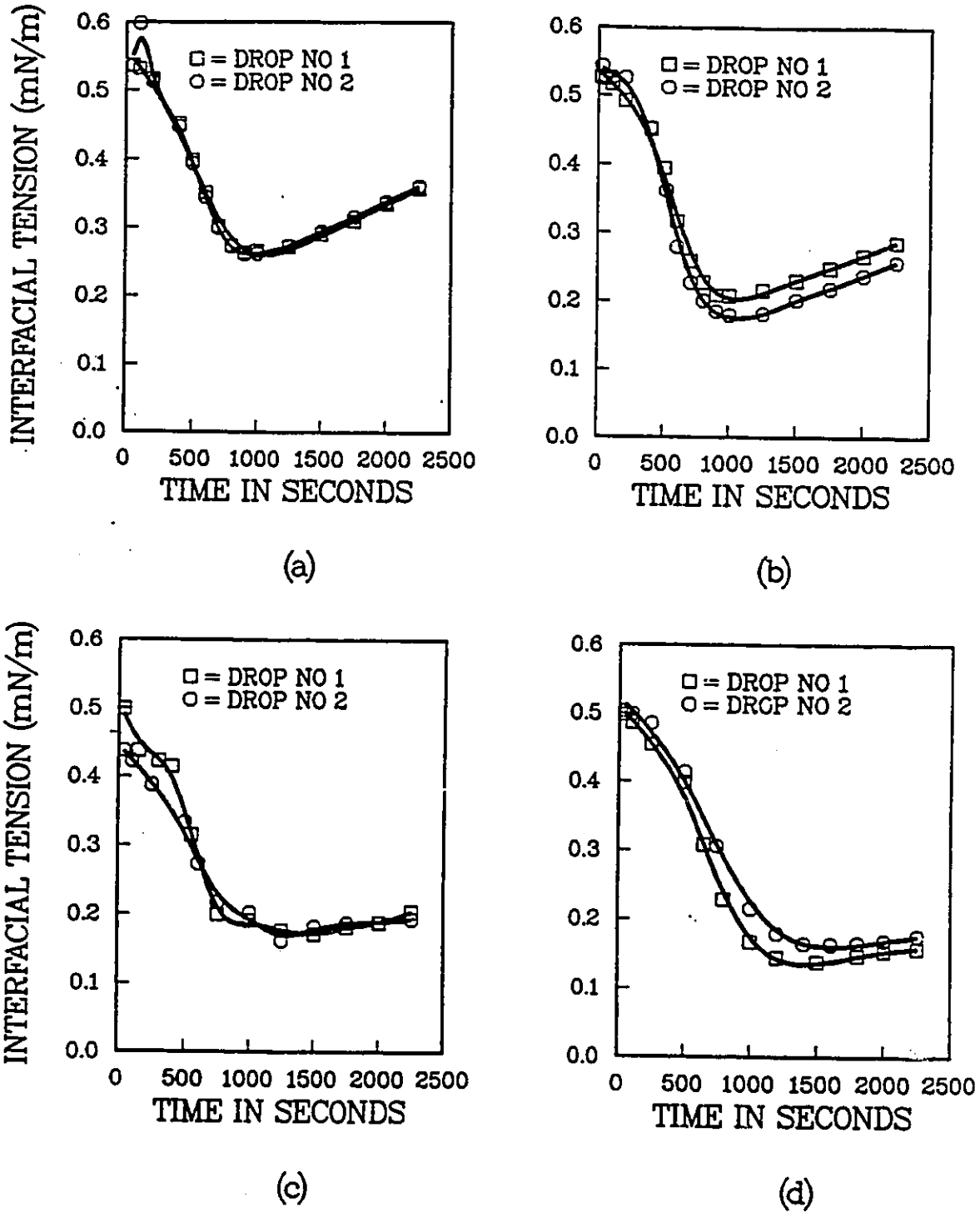

Figure 4.2: IFT vs Time for Linoleic Acid ((a) 1 mM; (b) 10 mM; (c) 20 mM; (d) 100 mM) in Light Paraffin Oil in contact with 25 mM NaOH solution at 25° C

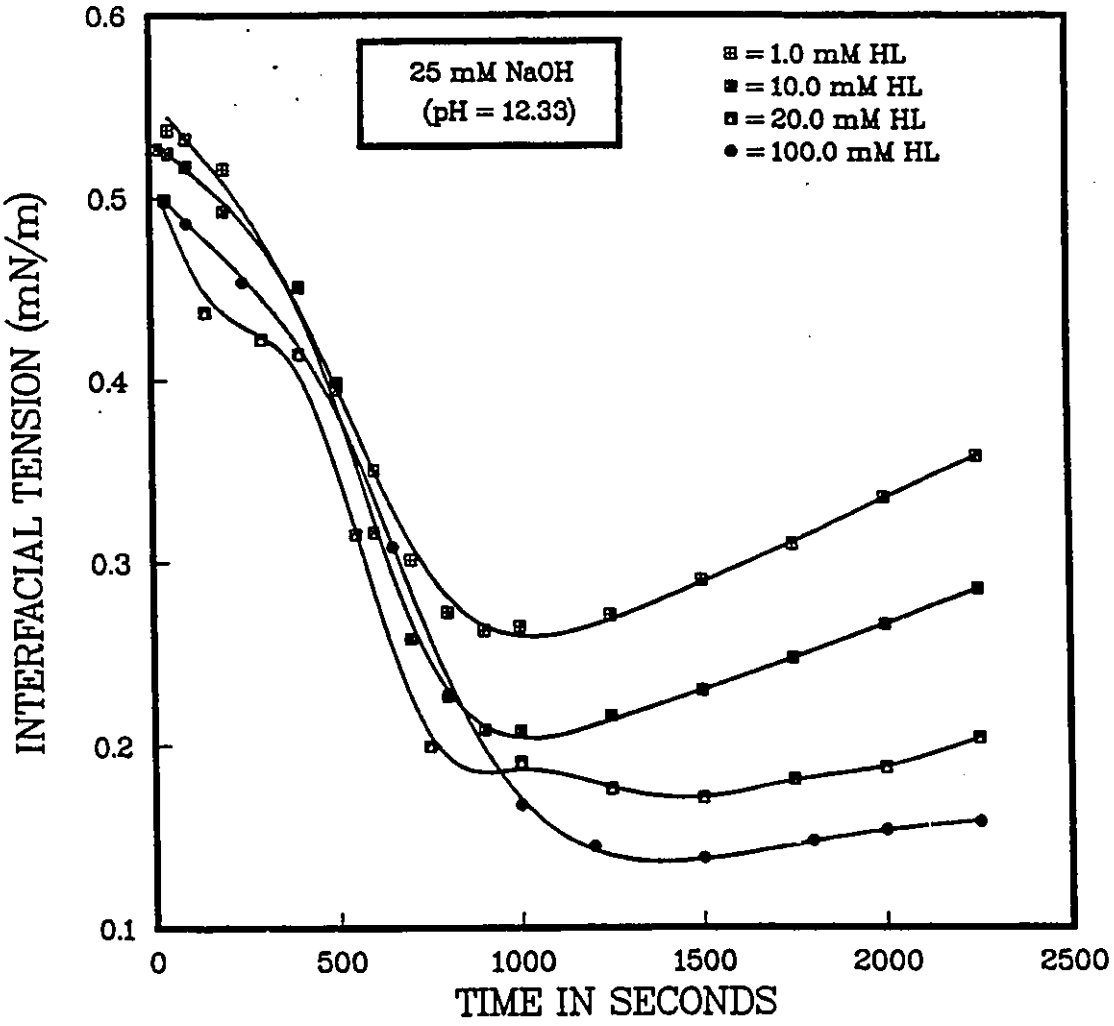

Figure 4.3: Effect on Transient IFT behavior of concentration of Linoleic Acid in Light Paraffin Oil in contact with 25 mM NaOH solution at 25° C.

At a caustic concentration of 1.25 mM, we find in Fig. 4.5(a) that the IFT started with a low value of 0.52 mN/m after 50 seconds of spinning, and that it increased sharply to attain a maximum of 1.30 mN/m, followed by a decrease to an equilibrium value of 0.85 mN/m. When caustic concentration in the aqueous phase of 2.5 mM was used (Fig. 4.5(b)), the initial IFT was 0.4 mN/m and it gradually increased to 0.78 mN/m in 1800 seconds. For an aqueous phase of 12.5 mM NaOH (Fig. 4.5(c), the IFT obtained after a short time of spinning was 0.5 mN/m. With this aqueous composition, the IFT did not increase appreciably from the minimum even at extended times. The trend observed at a caustic concentration of 25 mM (Fig. 4.5(d) was similar to that found at 12.50 mM. However, the minimum was slightly higher at 0.20 mN/m and it was attained at a contact time of 1000 seconds. At concentrations up to 50 mM NaOH in the aqueous phase, the transient IFT exhibited the same trend as found using 25 mM, but with higher absolute values. With further increases in the caustic concentration up to 500 mM, the trend in the dynamic IFT was markedly different. For example, at a caustic concentration of 100 mM (Fig. 4.5(f)), the initial IFT was 0.4 mN/m. Then it started to increase only after 300 seconds to attain a maximum near 0.54 mN/m after a contact time of 700 seconds. Fig. 4.5(g) shows similar trends when the caustic concentration of 250 mM was used. In Fig. 4.5(h), 500 mM NaOH was used and no characteristic IFT minima was observed. The tension rose steadily from an initial value of 0.65 mN/m to 1.5 mN/m attained after 1800 seconds.

The effects of varying caustic concentrations on dynamic IFT of acidic oil/caustic systems have been studied by various researchers [3,51]. It has been shown that low IFTs are obtained only over a narrow range of caustic concentration (typically 2.5 to 25 mM). Chan and Yen [51] suggested that this behavior was influenced by the effective caustic concentration at which the interfacial pH approached the pK_a value of the acid present in the oil. Fig. 4.7 shows the equilibrium IFT (obtained at extended spinning time) as a function of NaOH concentration. As can be seen in Figs. 4.6 and 4.7, the lowest IFT values were obtained with a sodium hydroxide concentration of 12.5 mM. This indicates that linoleic acid has a pK_a much lower than 12 (the pH of a 12.5 mN NaOH solution). At caustic concentrations below 12.5 mM, the acid species present at the interface are largely and completely ionized resulting in a high initial accumulation of the surface-active soap anions. Since these surface-active anions are charged, an electrical double layer is formed at the interface and this tends to stabilize the adsorbed ions. The result is a relatively large barrier to desorption of the anions into the aqueous phase, which explains the decrease in IFT at extended contact times.

For NaOH concentrations above 12.5 mM, surface inactive soap complexes are formed as a result of chemical reaction between the active anions and excess sodium ions [26,51,63]. This results in a gradual loss of the adsorbed anions and a subsequent decrease in the resistance to desorption. Consequently, the IFT increases at extended spinning times. In the case of linoleic acid systems, 250 mM is the critical

caustic concentration at which significant desorption of the soap anions occurred.

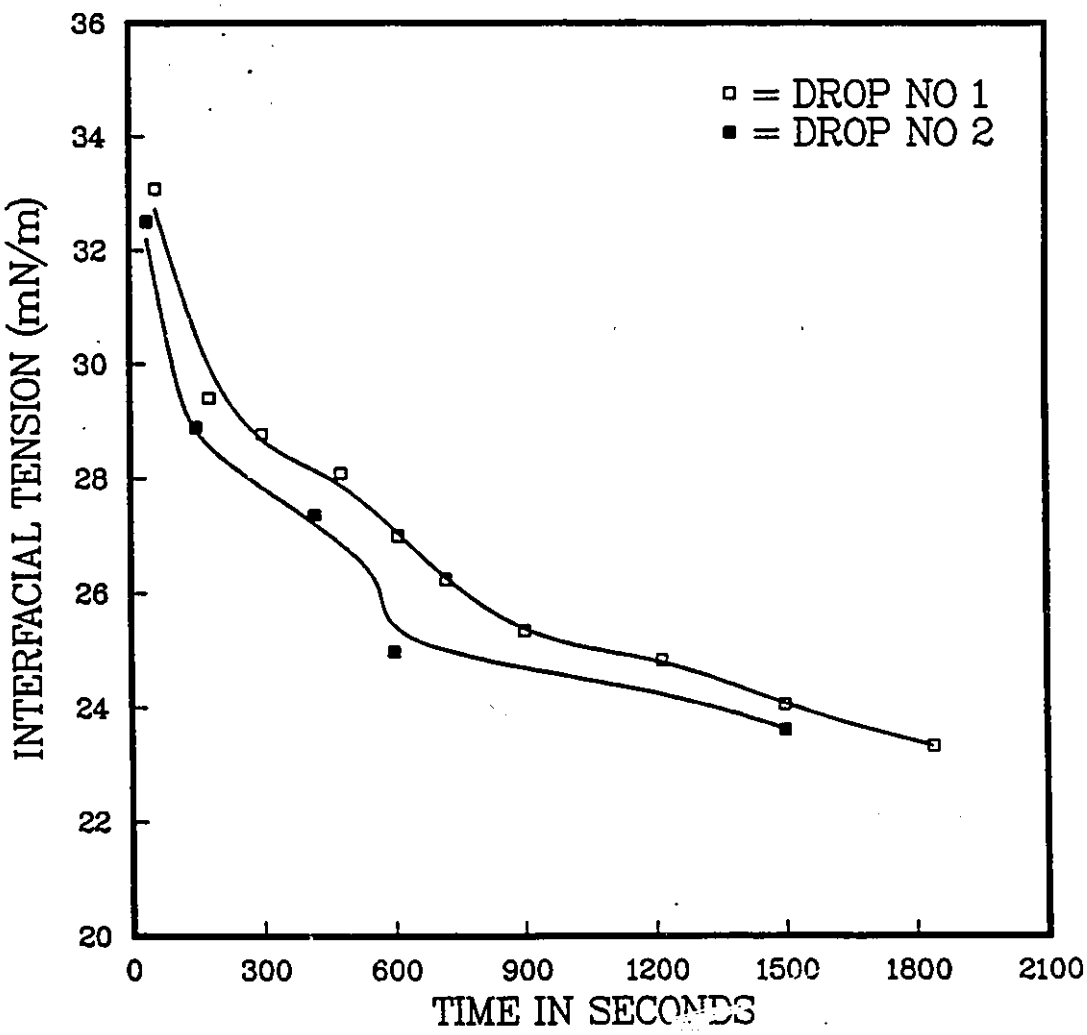

Figure 4.4: IFT vs Time for 10 mM Linoleic Acid in Paraffin Oil in contact with Distilled Water at 25° C.

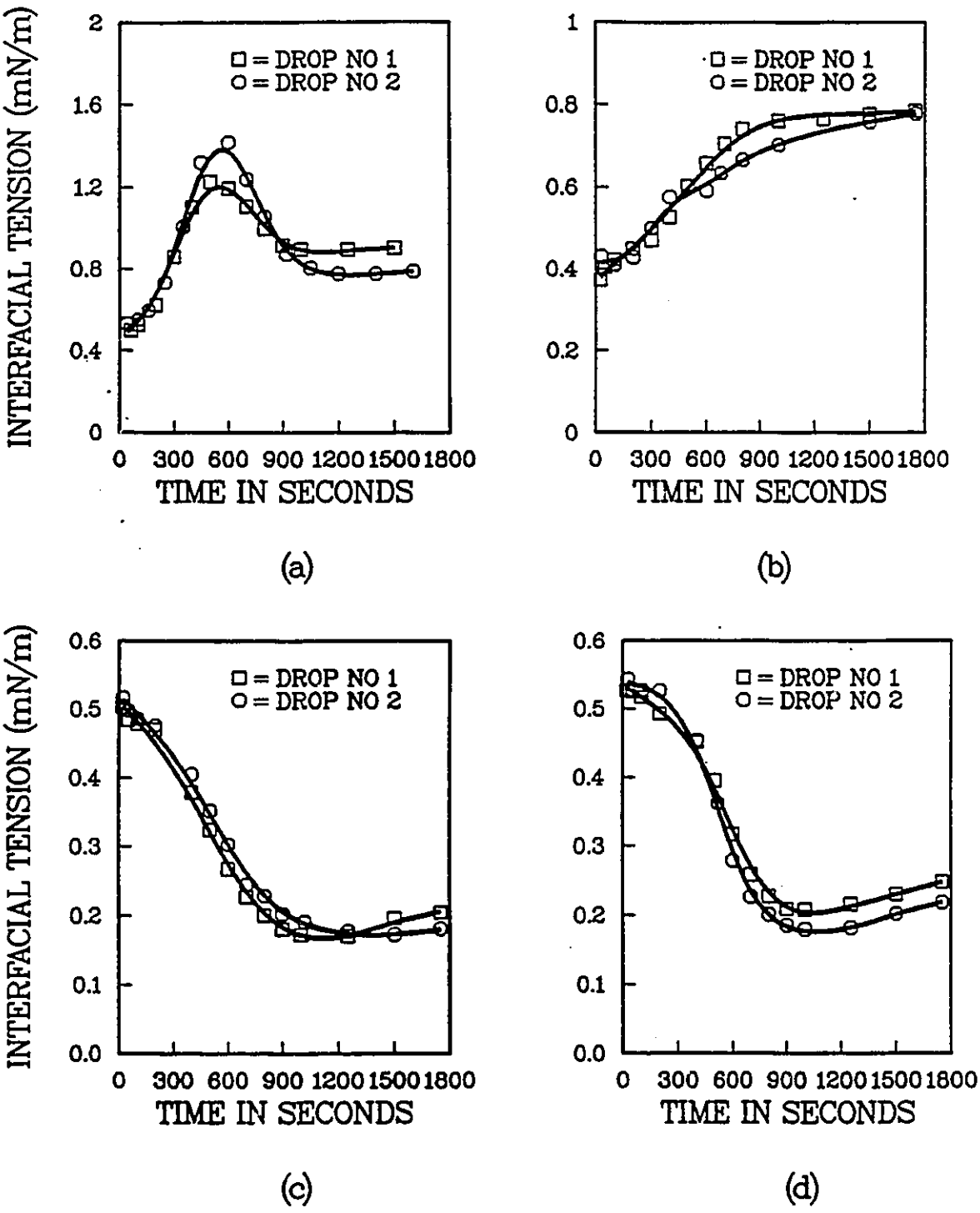

Figure 4.5: IFT vs Time for 10 mM Linoleic Acid in Paraffin Oil in contact with Alkaline Solutions at 25° C: (a) 1.25 mM; (b) 2.5 mM; (c) 12.5 mM; (d) 25 mM.

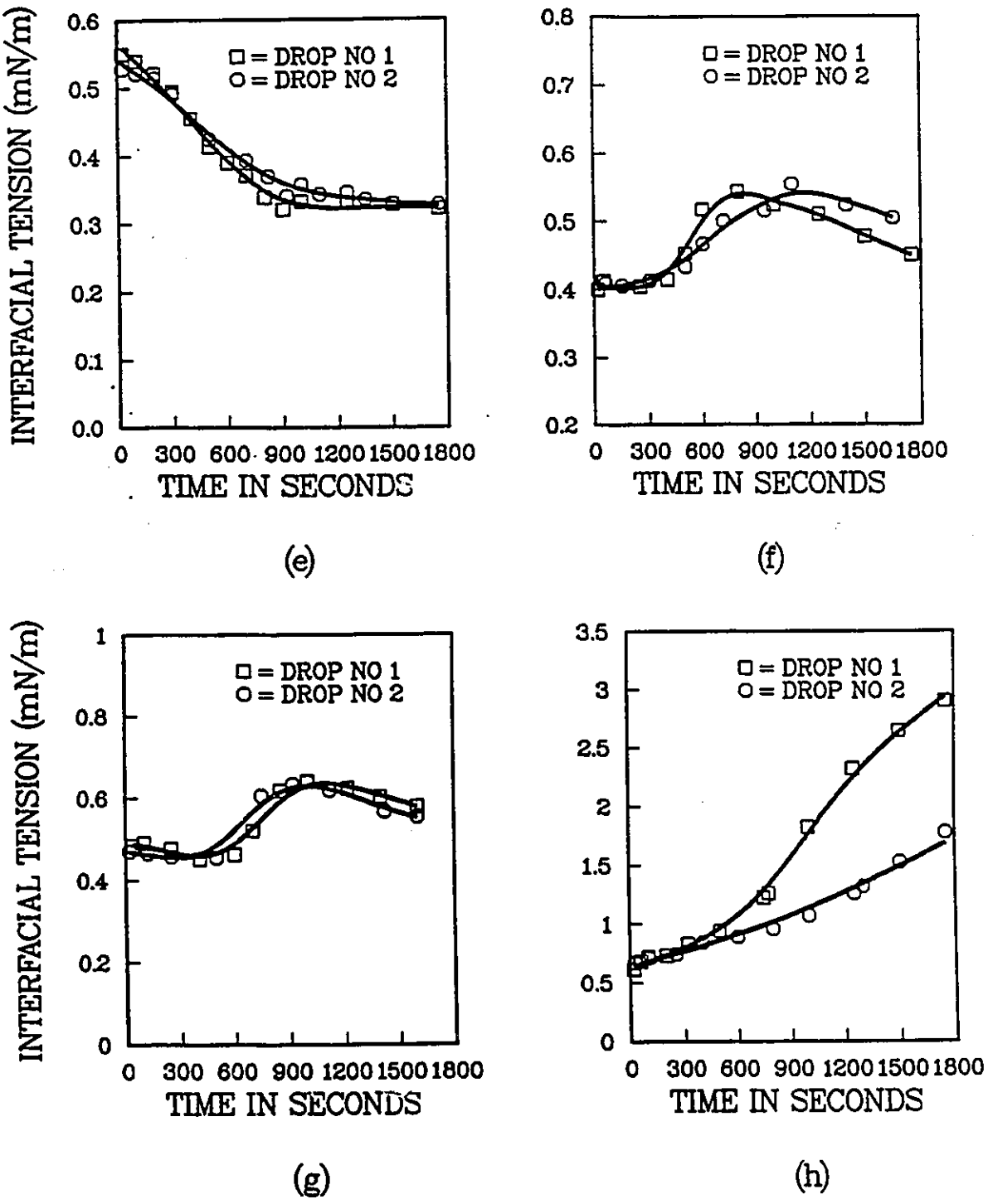

Figure 4.5: Continued (e) 50 mM; (f) 100 mM; (g) 250 mM; (h) 500 mM.

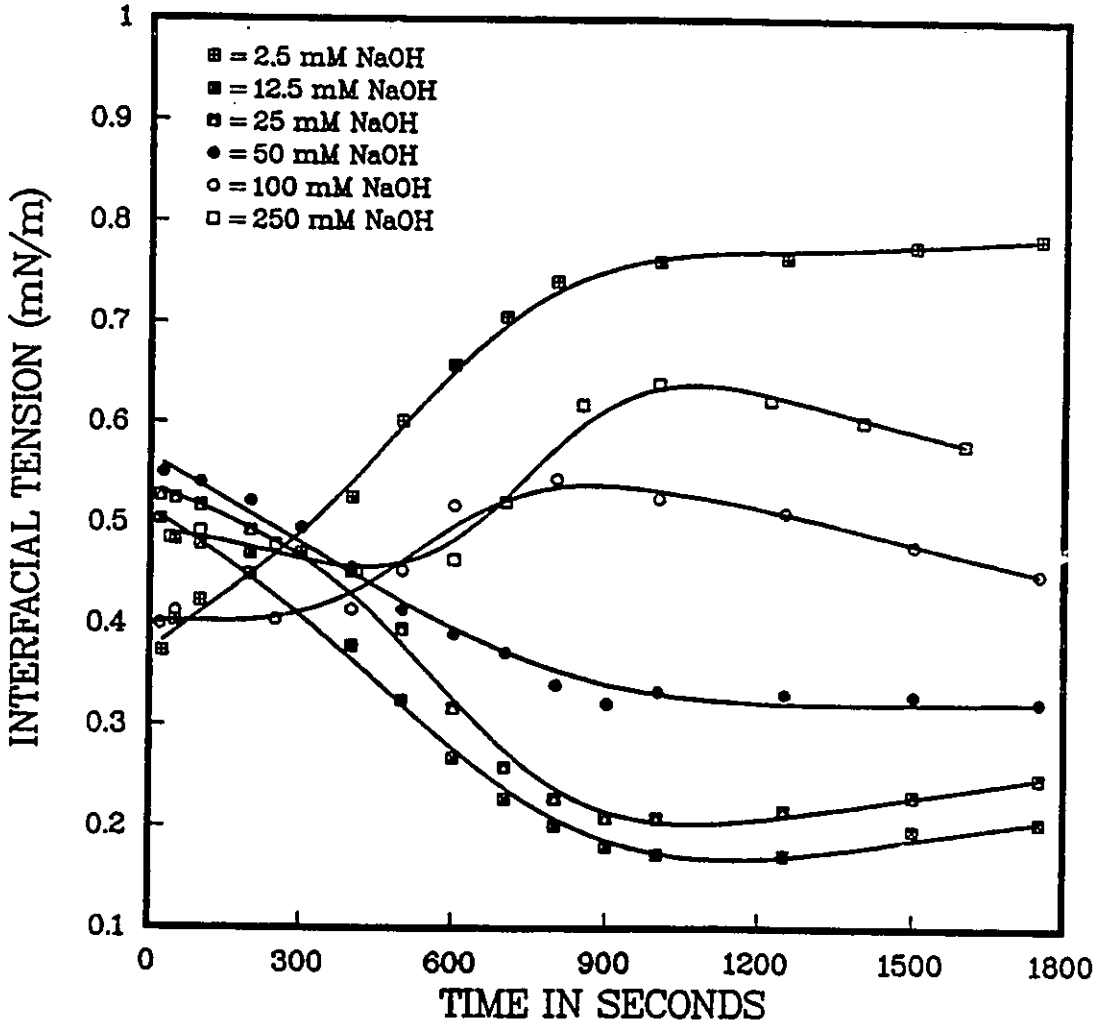

Figure 4.6: Effect on Transient IFT behavior of 10 mM Linoleic Acid in contact with NaOH solutions at 25° C.

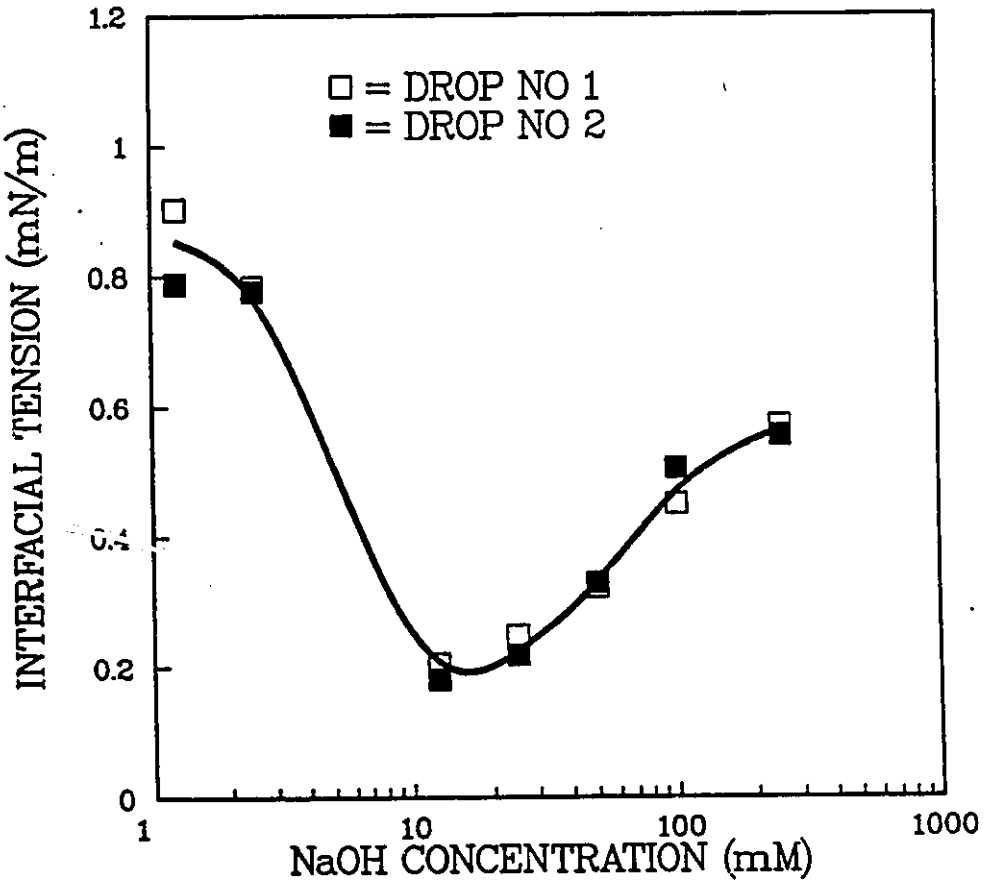

Figure 4.7: Variation of IFT with NaOH Concentration for 10 mM Linoleic Acid in Paraffin Oil at 25° C.

4.3 Interfacial Behavior of Polymer Solutions

4.3.1 Polymer Characteristics, Solubility and Phase Compatibility

PVA and PAM were tested separately for their solubility and phase compatibility in NaOH solutions. PVA is very soluble in water [75]. The temperature at which the resin dissolves varies considerably with its grade and with its degree of hydrolysis. The PVA used in this work has a minimum degree of hydrolysis of 87 % which explains its ready solubility in both hot and cold water. Preliminary experiments indicated that PVA does not dissolve completely in NaOH solution. Therefore, the PVA stock solutions were prepared in cold water using a low speed of agitation. Caustic-polymer solutions were then prepared first by adding a predetermined amount of the polymer stock solution to a measured amount of stock NaOH solution, and later adding distilled water to achieve the desired working concentrations.

PAM on the other hand is soluble in water in all proportions [76]. Tests were performed with two different molecular weights. It was observed that molecular weight does not appear to affect the solubility in water. PAM used in this study was non-ionic and had a molecular weight in the range of 5×10^6 to 6×10^6. Under alkaline conditions, the extent of dissolution of this polymer was very slow even at high mixing speed. To avoid any mechanical degradation resulting from

a high mixing rate at extended times, PAM solutions were prepared using the same procedure as for PVA solutions. The viscosity data presented in Tables A5–A8 indicate the absence of any appreciable synergistic effects resulting from the addition of polymers to NaOH solutions.

4.3.2 Interfacial Activity of Polymers

The interfacial activity of the two polymers was determined by measuring the IFT of the polymer solutions (in water) against 10 mM linoleic acid in paraffin oil. For the viscosity range employed in this work, it was sufficient to limit the PVA concentration to a maximum of 3.0 % by weight, while for PAM the limiting concentration was 0.3 % by weight.

Polyvinyl Alcohol

The interfacial data for PVA have been grouped into a composite plot which is Fig. 4.8. As can be seen from this figure, the PVA exhibited an interfacial activity significantly higher than that of distilled water. For example, a 0.1 % solution had an initial IFT value of 18 mN/m which decreased gradually to an equilibrium value of 12.5 mN/m in 2000 seconds of spinning. This decreasing trend in dynamic IFT was observed for all the other PVA concentrations studied. However, at high PVA concentration, lower IFT values were measured at all contact times. This lowering

in IFT was less pronounced at concentrations above 2.0 % and at longer spinning times. The lowest IFT for a 2.0 % PVA solution was 8.15 mN/m, whereas for the 3.0 % solution it was only 7.8 mN/m.

Polyacrylamide

The interfacial data for PAM are presented in Fig. 4.9. It is evident from Figs. 4.8 and 4.9 that PAM solutions show the same transient IFT behavior as for PVA. IFT values for the former were relatively higher in magnitude. A solution of 0.05 % by weight PAM contacting a 10 mM linoleic acid solution had an initial IFT value of 21 mN/m. The IFT subsequently decreased gradually to reach a value of 18 mN/m after a contact time of 2000 seconds. As the polymer concentration in the aqueous phase increased, the IFT values decreased while the decreasing trend remained unchanged. At PAM concentration of 0.3 %, the IFT obtained after 60 seconds of spinning was 16.3 mN/m, and it dropped to 13.4 mN/m after a contact time of 2000 seconds. In Figs. 4.10-4.11, we have plotted the equilibrium IFT for the working polymer concentrations. As described earlier, IFT values for PVA systems were consistently lower than those obtained for PAM.

The transient IFT behavior of PVA and PAM solutions in contact with 10 mM linoleic acid solutions can be explained in terms of the chemical nature of the polymers and their rheological behavior. Being surface-active, the polar heads of

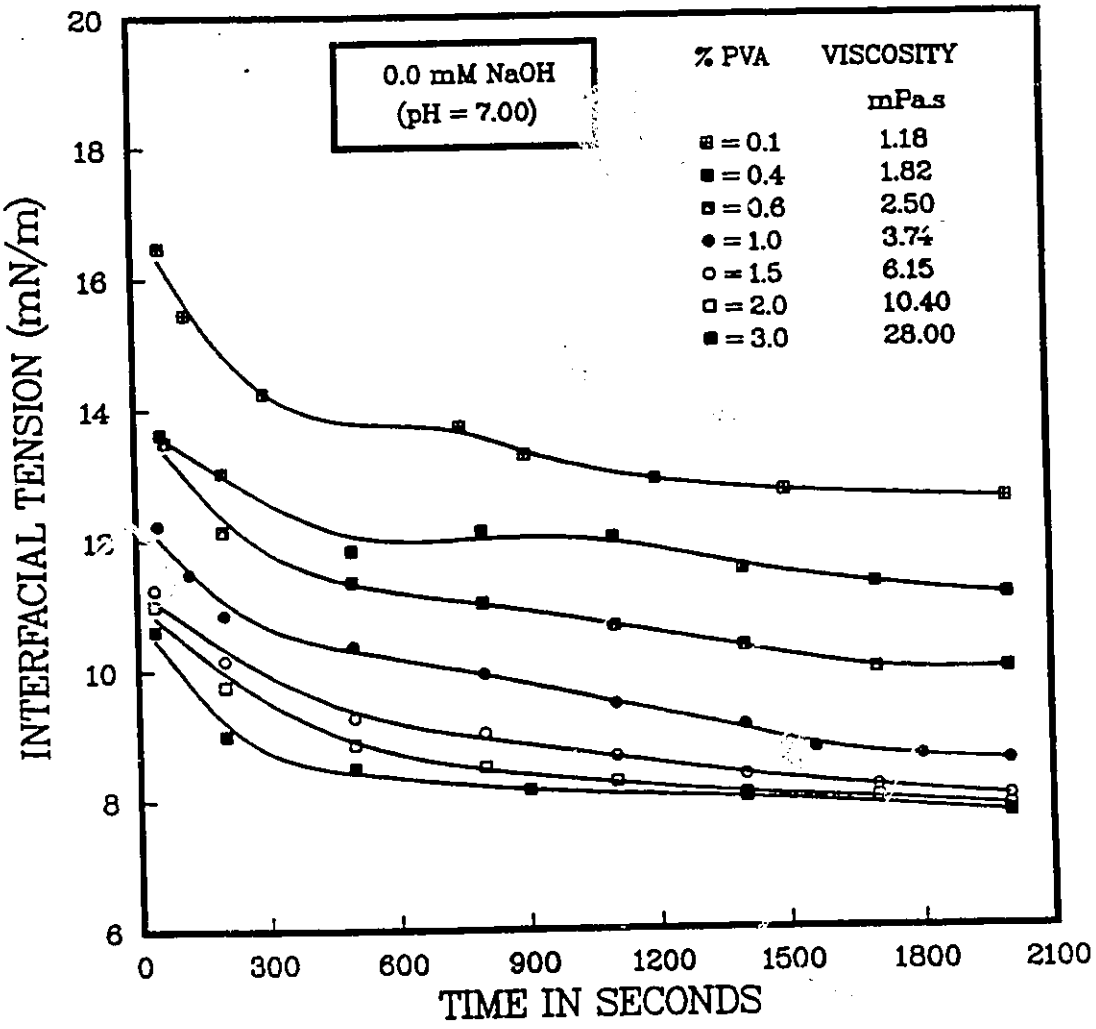

Figure 4.8: Transient IFT behavior of 10 mM Linoleic Acid in Paraffin Oil in contact with Polyvinyl-Alcohol Solution at 25° C.

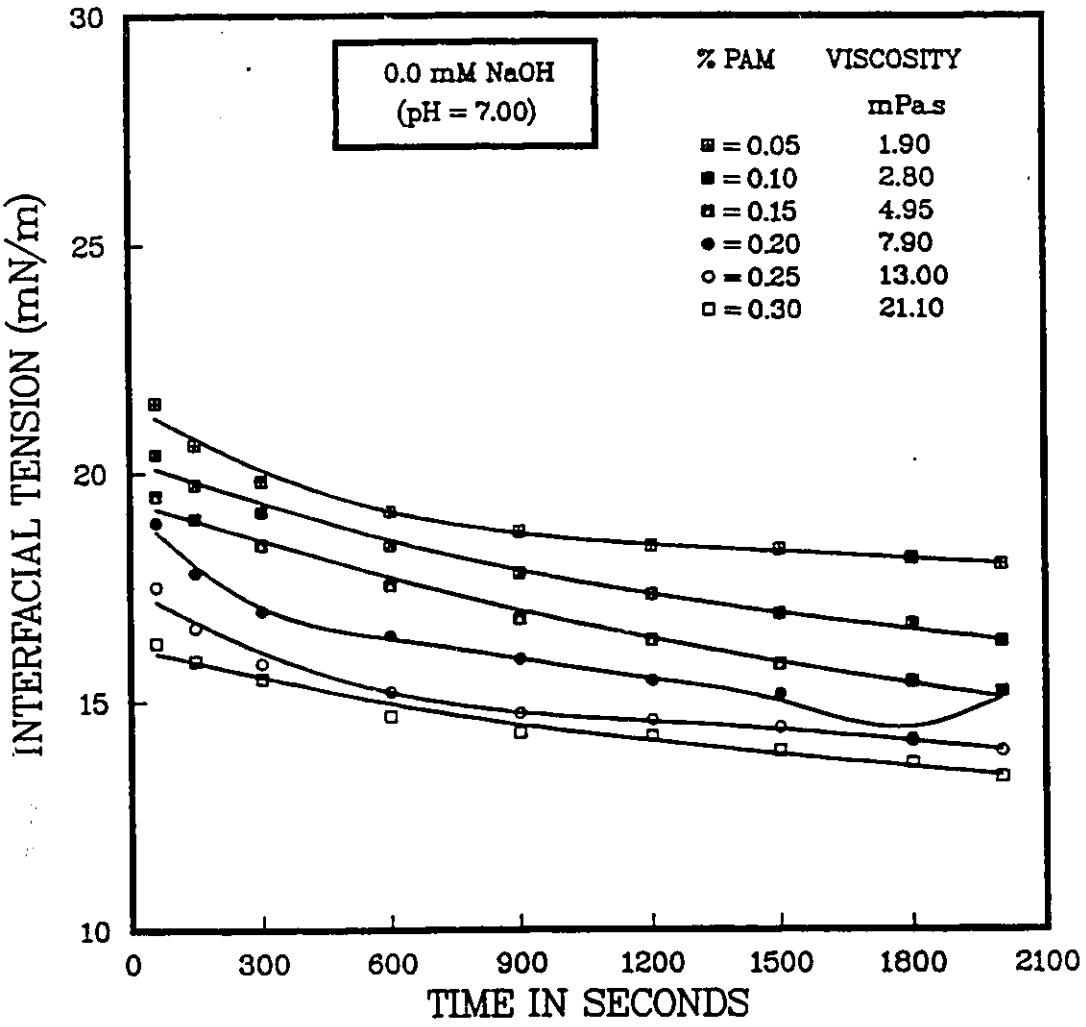

Figure 4.9: Transient IFT behavior of 10 mM Linoleic Acid in Paraffin Oil in contact with Polyacrylamide Solutions at 25° C.

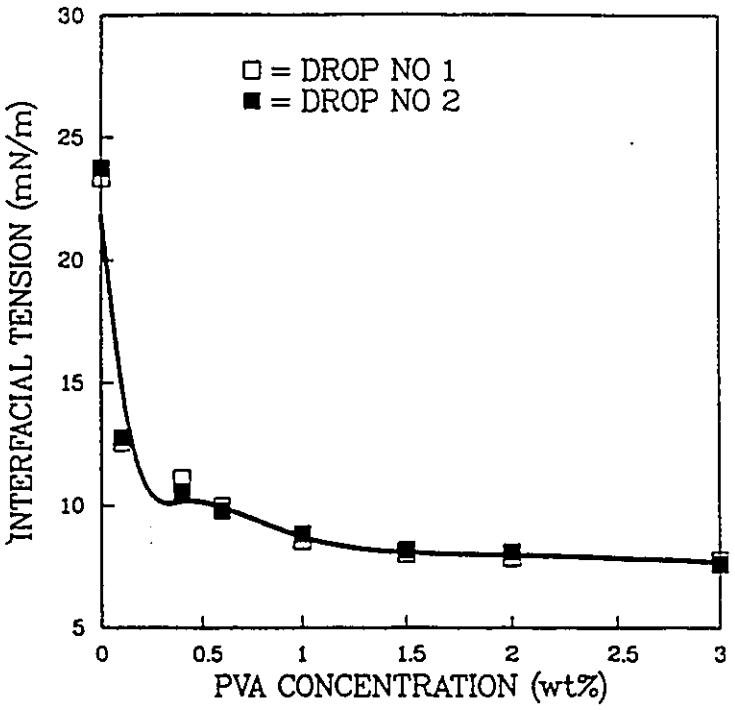

Figure 4.10: Equilibrium IFT vs Polyvinyl Alcohol Concentration for 10 mM Linoleic Acid in Paraffin Oil System.

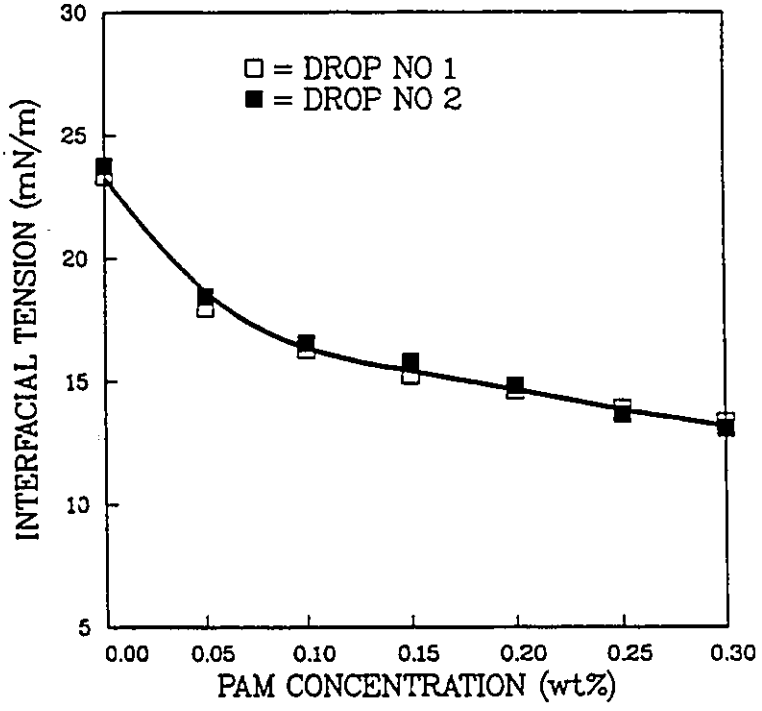

Figure 4.11: Equilibrium IFT vs Polyacrylamide Concentration for 10 mM Linoleic Acid in Paraffin Oil System.

polymer chains tend to adsorb at the oil-water interface. This results in a lowering of the IFT according to Gibbs Law. As can be seen from Fig. 4.10, there is no further reduction in IFT at concentrations above 2 % for PVA. At this polymer concentration, the oil-water interface is saturated and a molecular layer of adsorbed polymer is formed. This physical adsorption, which results in the formation of a polymer film at the interface, depends strongly on the molecular weight, the intermolecular forces, and the intramolecular forces [4,5]. Intermolecular cohesive forces also depend on the polarity of the surface-active species present in the polymer. Structurally, PVA can be described as a polyhydric alcohol with hydroxyl groups on alternate carbon atoms [77,78]. When these side groups are adsorbed at the interface, the resulting film has a flat molecular configuration [79]. This results in a more completely covered interface. Conversely, adsorbed films of PAM will exhibit an uneven molecular configuration due to relatively large steric effects. The above phenomena can explain the significant differences in the transient IFT behavior for PVA and PAM. The experimental IFT data suggest that the polymer (alone) dissolved in the aqueous phase exerts a considerable interfacial activity which must be taken into account when evaluating the behavior of polymer-caustic systems.

4.3.3 Transient IFT Behavior of Oil/Polymer-Caustic Interfaces

Interfacial tension data for a broad range of polymer-caustic solutions against 10 mM linoleic acid in paraffin oil were measured. Five different caustic concentrations (up to a maximum of 250 mM) were involved in this phase of the study. The polymer concentrations of these caustic solutions were maintained at levels necessary to achieve a predetermined viscosity enhancement. The complete set of interfacial data for all caustic levels and for all polymer concentrations are presented in Figs. 4.12 to 4.21. The resulting IFT data have been plotted as a function of interfacial age for the various polymer-caustic formulations. For each plot, the data points are the average values from two replicate experiments. The percentage error in the IFT measurement for the same system was generally less than 5 %, which compares quite well with the results of previous researchers [25,31].

IFT Data for PVA/Caustic Systems

The IFT data for PVA at different NaOH concentrations are shown in Figs. 4.12–4.17. Fig. 4.12 gives the dynamic IFT plot when 10 mM linoleic acid in paraffin oil is contacted with 2.5 mM NaOH solutions containing varying PVA concentrations (i.e. different viscosities). The pH indicated in Fig 4.12, as well as in other similar figures, refers to the pH of the polymer-free NaOH solutions. The addition of

increasing amounts of PVA to 2.5 mM NaOH appeared to alter the previously observed increase in IFT with contact time. At a polymer concentration of 0.3% (i.e. viscosity of 1.65 mPa.s), the IFT increased slowly but steadily from an initial value of 0.4 mN/m to about 1.52 mN/m attained after 2000 seconds. The IFT values obtained following the addition of PVA were marginally higher than corresponding tension values of polymer-free 2.5 mM NaOH. When the polymer concentration was raised to 0.6 %, giving a bulk viscosity of 2.50 mPa.s, the rate of increase in IFT was somewhat higher and the maximum tension values rose to 3.02 mN/m after an interfacial age of 2000 seconds. With further increase in the polymer concentration, from 0.6 % to 1.8 %, the initial rise in tension values was rather sharp. Thereafter, the IFT rose slowly to an equilibrium value of about 4.13 mN/m. As can be seen in Fig. 4.12 , the effects of polymer addition (viscosity) are particularly evident at low concentrations (< 0.9 %). Beyond this concentration, the effects were less significant.

For 12.5 mM NaOH solution, Fig. 4.13 shows the effects of the addition of PVA additives on transient IFT behavior. A comparison with the polymer-free caustic solution reveals that the dynamic IFT exhibited a particularly distinguishable trend. For instance, the initial values were lower than that of the 12.5 mM NaOH solution. The dynamic IFT minima were reached at shorter times, and a characteristic increase in IFT was observed thereafter.

For the polymer-free 12.5 mM NaOH, the initial IFT was 0.5 mN/m which

later settled to a minimum tension of 0.1722 mN/m. When PVA concentration of 0.3 % was added, the minimum in IFT was higher and this was attained much faster, at an interfacial age of 160 seconds Thereafter, the boundary tension slowly increased to about 0.352 mN/m after a contact time of 2000 seconds. In general (as Fig. 4.13 depicts), as the aqueous phase viscosity increased (i.e. increasing polymer concentrations), the minimum IFT increased marginally and was reached at almost the same time for all of the polymer concentrations used. Therefore, the subsequent rate of increase in IFT was strongly dependent on the prevailing polymer concentration. The IFT at any given contact time and for any given polymer concentration differed considerably from the values obtained in the absence of polymer.

The transient IFT behavior of 25 mM NaOH (pH 12.33) solution containing varying PVA is plotted in Fig.4.14. The trends in dynamic IFT for this system are similar to the results described earlier for 12.5 mM NaOH. The only notable difference is the marginally higher tension values and the locations of the IFT minima. As the polymer concentration was increased, the minimum IFT value increased and this minimum was obtained at correspondingly shorter contact times. This observation is in line with the finding of Rubin and Radke [3] that the deeper the dynamic IFT minimum is, the later it appears. Fig. 4.15 shows the dynamic IFT data for a 10 mM linoleic acid oleic solution contacted with 125 mM NaOH solutions containing PVA. In the absence of polymer, 125 mM NaOH gave only

an increasing dynamic IFT trend (see Fig. 4.5 (f)). However, for the polymer-thickened solutions, we observe a characteristic drop in IFT from an initial value of 0.4 mN/m to a minimum value near 0.22 mN/m. This minimum value was the same for all polymer concentrations and it occurred after about 750 seconds of spinning. Beyond this minimum, the subsequent increase in IFT depended on the prevailing PVA concentration. From Fig. 4.16 we can see that there is practically no difference in the IFT data for 250 mM NaOH containing PVA and even the trends are identical to those obtained for the 125 mM caustic/PVA system.

IFT Data for PAM/Caustic Systems

The IFT data for PAM/caustic solutions are shown in Figs. 4.17–4.21. IFT values for PAM/2.5 mM NaOH solutions (Fig. 4.17) were lower than the corresponding figures for polymer-free 2.5 mM NaOH solutions. Unlike the slightly increasing IFT/time trends of Fig. 4.5(b), the addition of PAM did not produced any significant change in the IFT even extended contact times. In a sharp contrast to the behavior of the 2.5 mM NaOH/PAM system, Fig. 4.18 shows that 12.5 mM NaOH containing varying amounts of PAM produced a characteristic dynamic IFT minimum near 0.15 mN/m which was independent of the PAM concentrations. At a low PAM concentration of 0.01 %, this minimum was attained after an interfacial age of 1150 seconds. Therefore, the IFT increased slightly to 0.239 mN/m attained after 2500 seconds of spinning. At higher PAM concentrations the minimum IFT

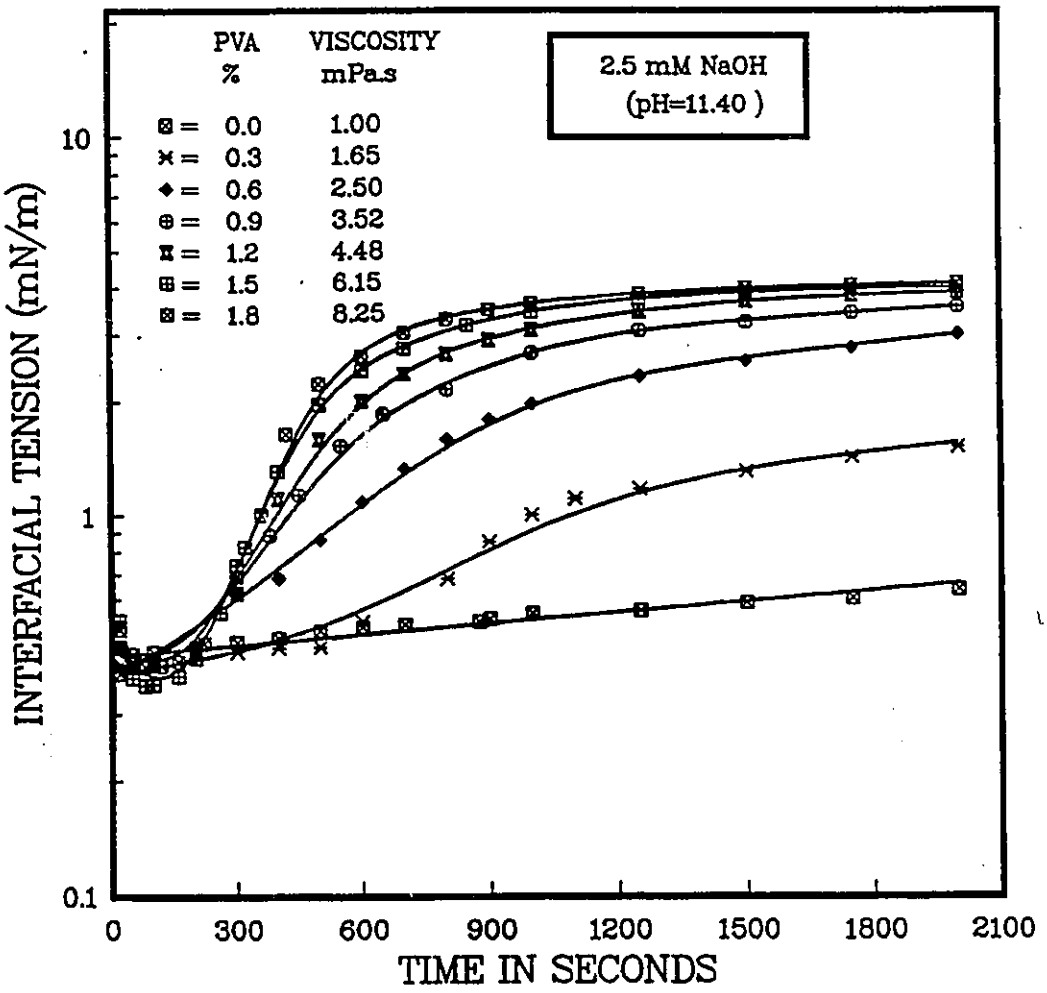

Figure 4.12: Effects of Polyvinyl-Alcohol (Aqueous Phase viscosity) on Transient IFT behavior of 10 mM Linoleic Acid in Paraffin Oil in contact with 2.5 mM NaOH Solution at 25° C.

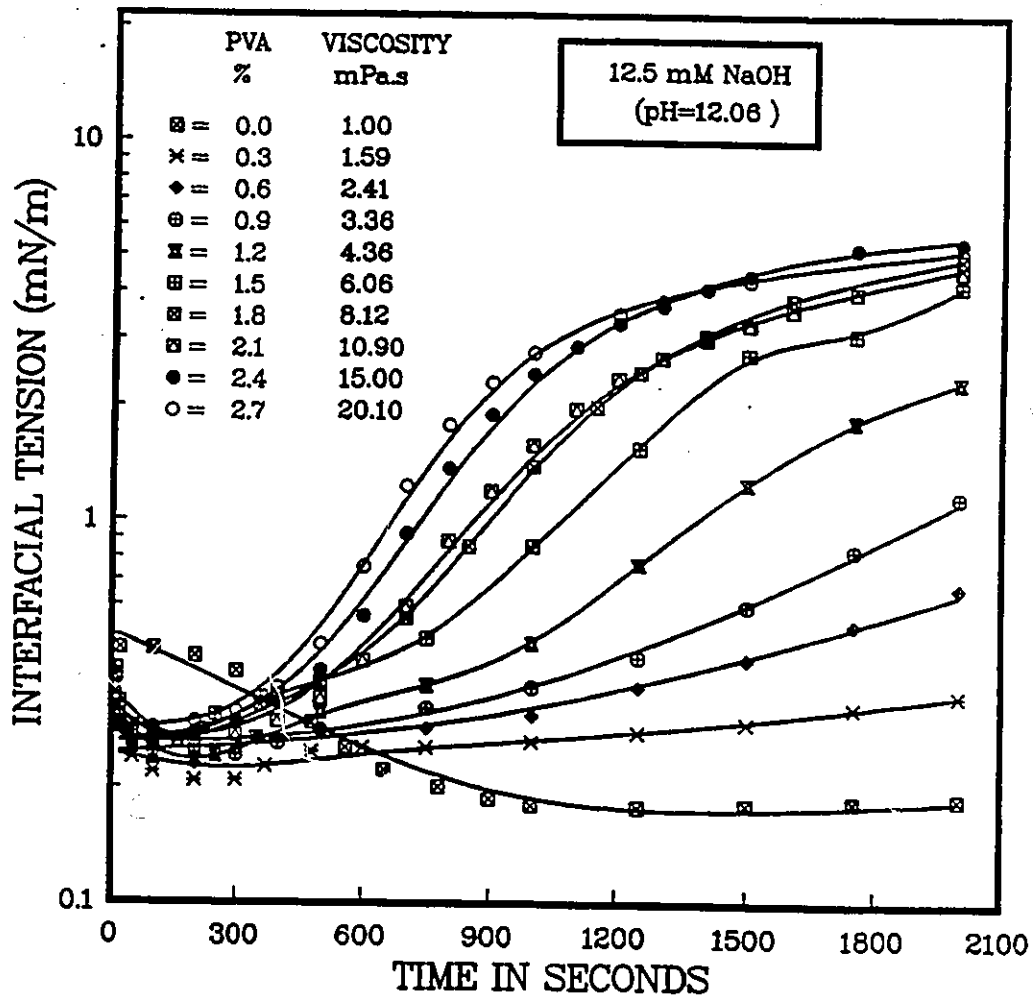

Figure 4.13: Effects of Polyvinyl-Alcohol (Aqueous Phase viscosity) on Transient IFT behavior of 10 mM Linoleic Acid in Paraffin Oil in contact with 12.5 mM NaOH Solution at 25° C.

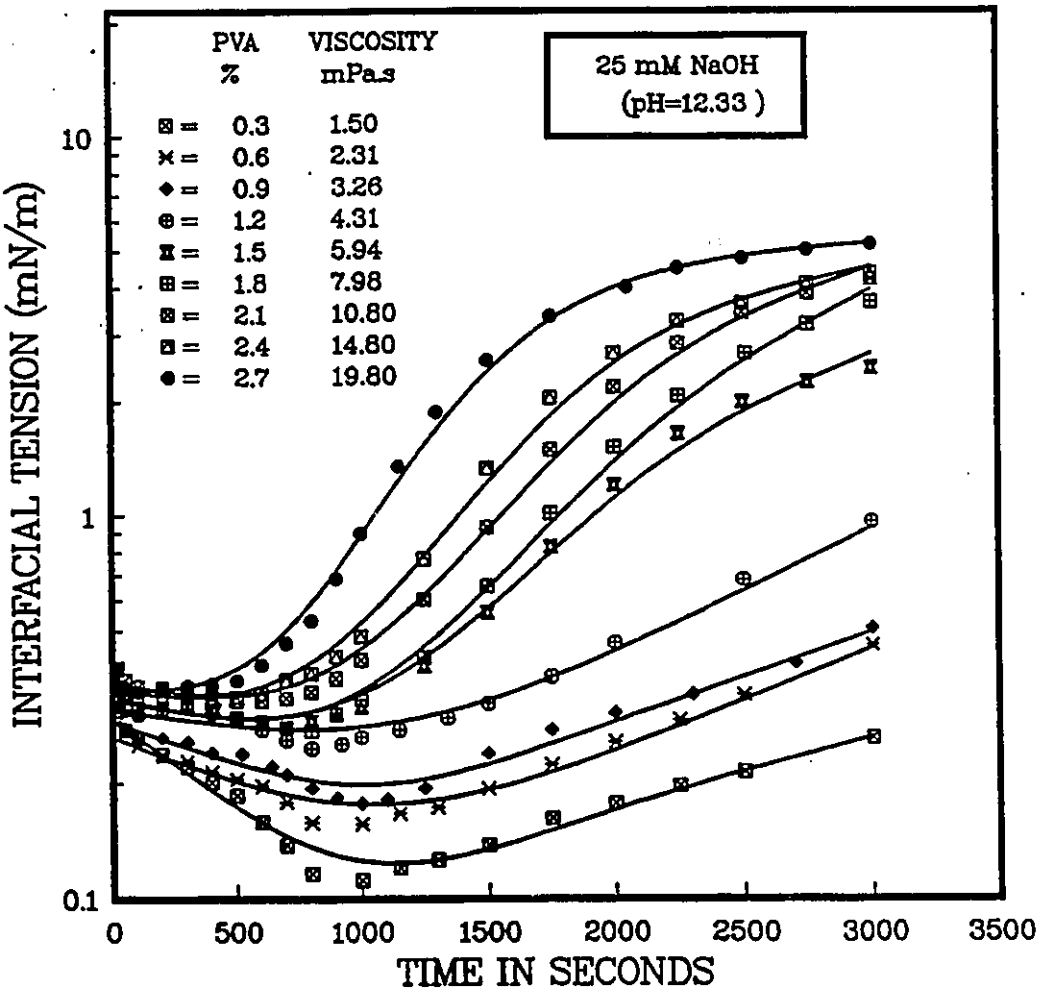

Figure 4.14: Effects of Polyvinyl-Alcohol (Aqueous Phase viscosity) on Transient IFT behavior of 10 mM Linoleic Acid in Paraffin Oil in contact with 25 mM NaOH Solution at 25° C.

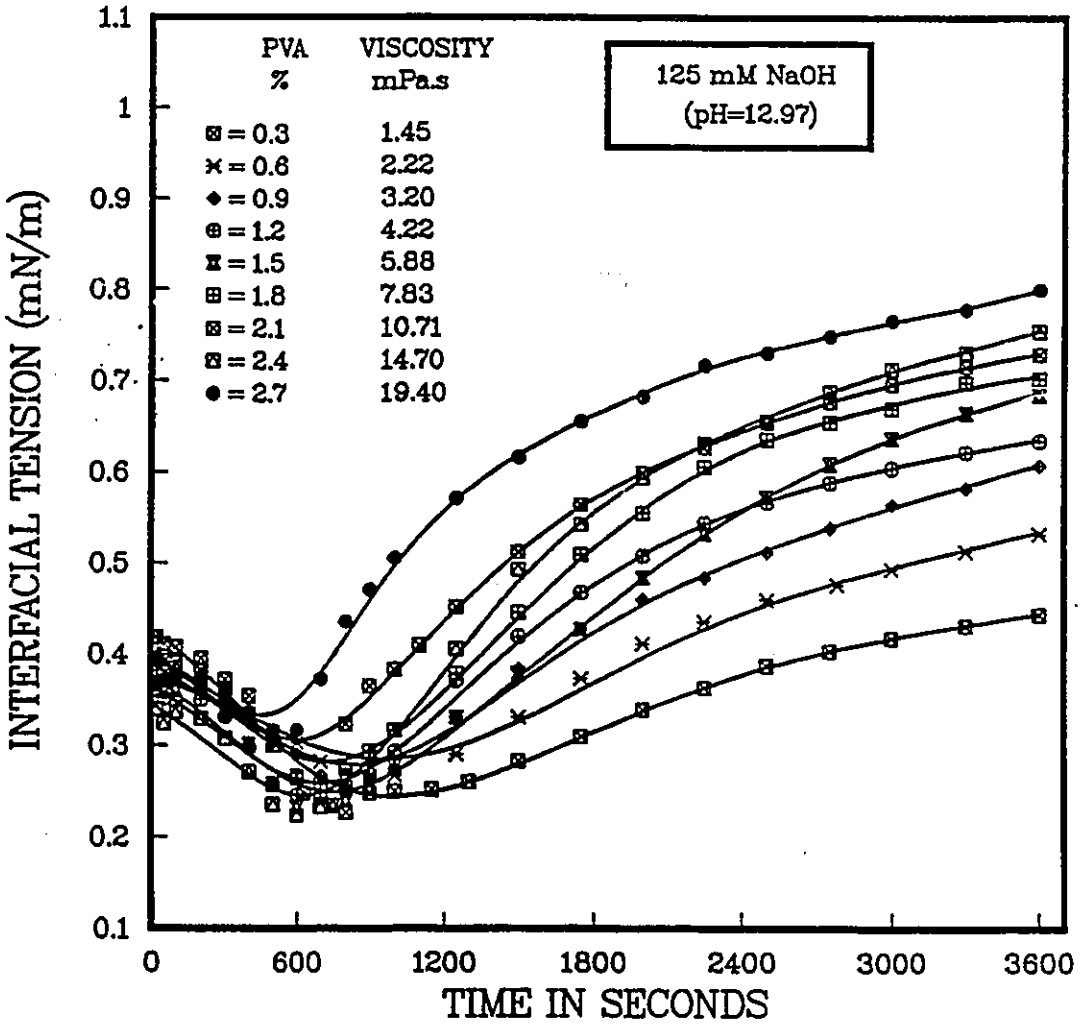

Figure 4.15: Effects of Polyvinyl-Alcohol (Aqueous Phase viscosity) on Transient IFT behavior of 10 mM Linoleic Acid in Paraffin Oil in contact with 125 mM NaOH Solution at 25° C.

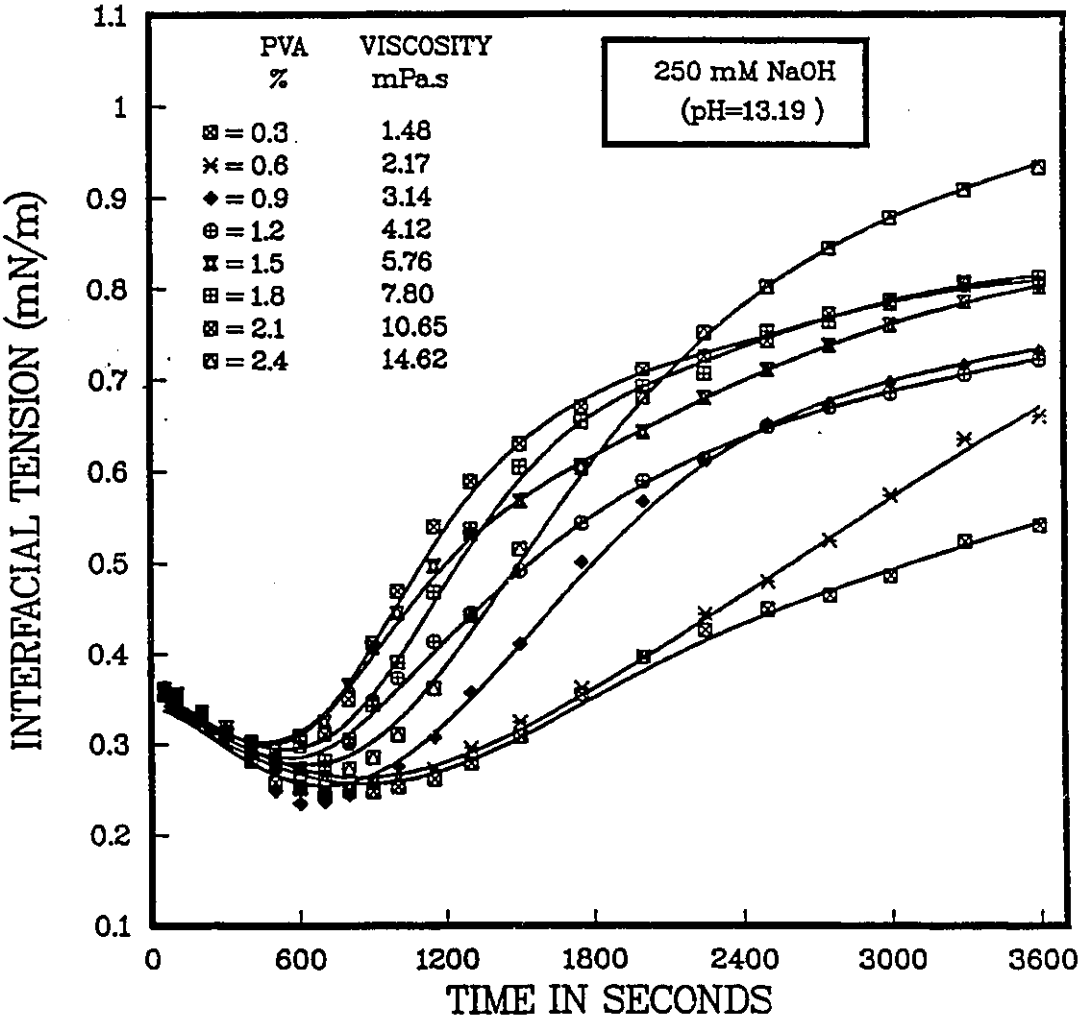

Figure 4.16: Effects of Polyvinyl-Alcohol (Aqueous Phase viscosity) on Transient IFT behavior of 10 mM Linoleic Acid in Paraffin Oil in contact with 250 mM NaOH Solution at 25° C.

was attained at shorter contact times, but beyond the minimum the rise in IFT was more pronounced. The trends in IFT/time data for PAM/25 mM NaOH system (see Fig. 4.19) were quite similar to those described above for the 12.5 mM NaOH system. For NaOH concentrations in the range of 125–250 mM, we find from Figs. 4.20 and 4.21 that characteristic IFT minima were again obtained when PAM was added to the caustic. However these minima occurred at later contact times when compared with the data obtained at lower NaOH concentrations. While the IFT minima occurred at an approximate contact time of 900 seconds (Fig. 4.20), the actual tension values showed a slight increase with higher PAM concentrations. Following the minima, the increase in IFT at longer contact times was also more pronounced at higher polymer concentrations. This observation is also true for 250 mM NaOH with PAM system (see Fig. 4.21).

Mechanism of Polymer/Caustic Interaction

The fact that those polymeric materials do possess surface-active properties has been highlighted in the preceding sections. However the surface activity of the polymeric material was shown to be somewhat reduced at higher polymer concentrations possibly due to steric effects. On the other hand, the incorporation of polymeric materials in NaOH solutions generally caused a small reduction in dynamic IFT until a characteristic minimum value was attained. This behavior was clearly manifested for both the PVA and PAM/caustic systems. Thus at early

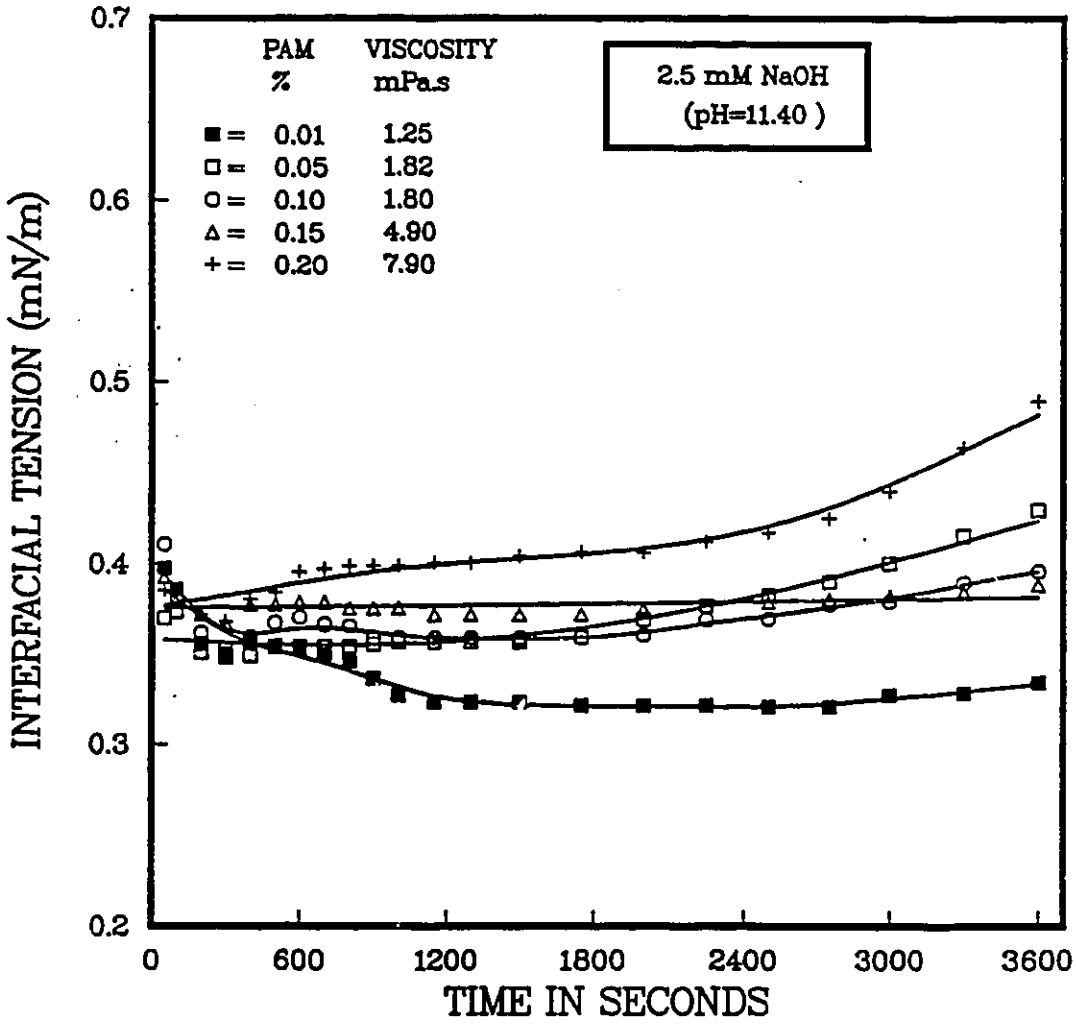

Figure 4.17: Effects of Polyacrylamide (Aqueous Phase viscosity) on Transient IFT behavior of 10 mM Linoleic Acid in Paraffin Oil in contact with 2.5 mM NaOH Solution at 25° C.

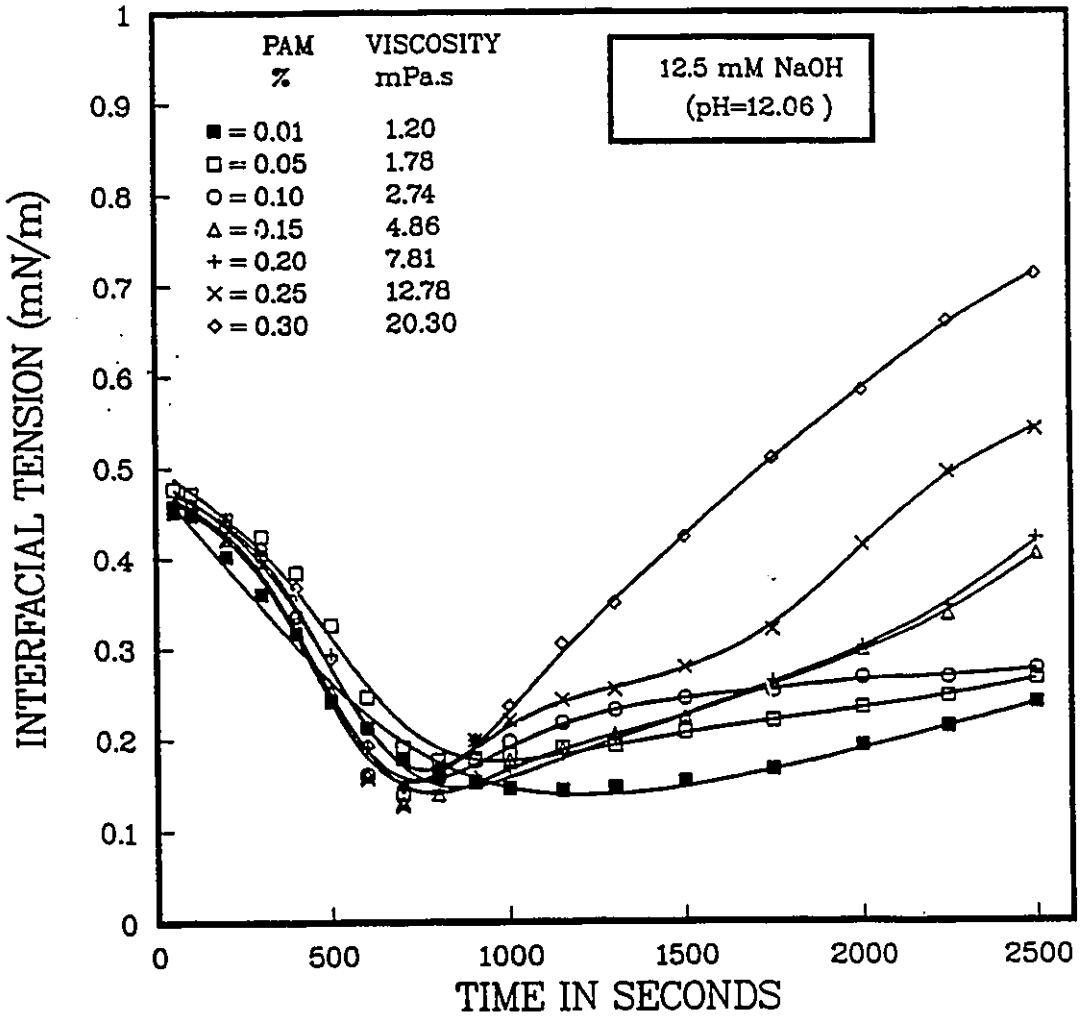

Figure 4.18: Effects of Polyacrylamide (Aqueous Phase viscosity) on Transient IFT behavior of 10 mM Linoleic Acid in Paraffin Oil in contact with 12.5 mM NaOH Solution at 25° C.

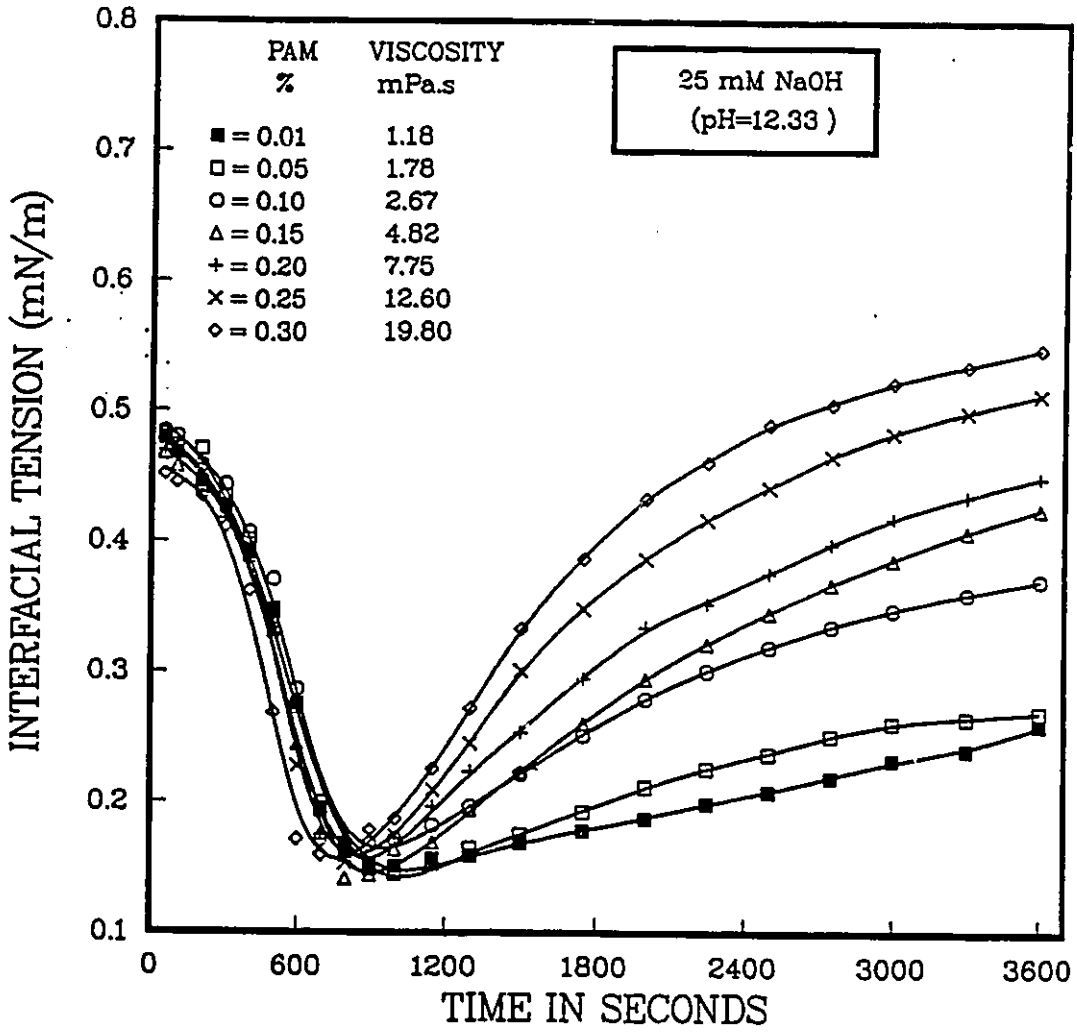

Figure 4.19: Effects of Polyacrylamide (Aqueous Phase viscosity) on Transient IFT behavior of 10 mM Linoleic Acid in Paraffin Oil in contact with 25 mM NaOH Solution at 25° C.

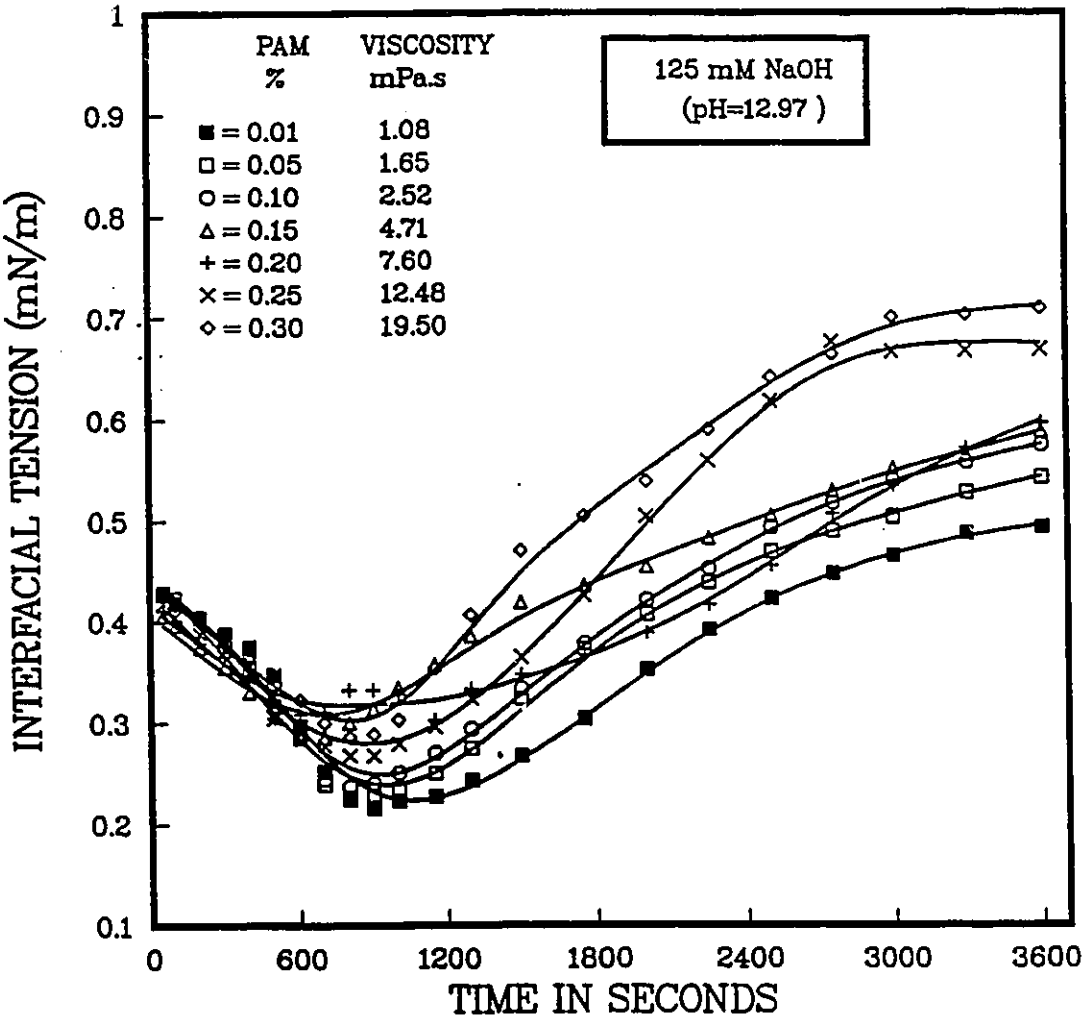

Figure 4.20: Effects of Polyacrylamide (Aqueous Phase viscosity) on Transient IFT behavior of 10 mM Linoleic Acid in Paraffin Oil in contact with 125 mM NaOH Solution at 25° C.

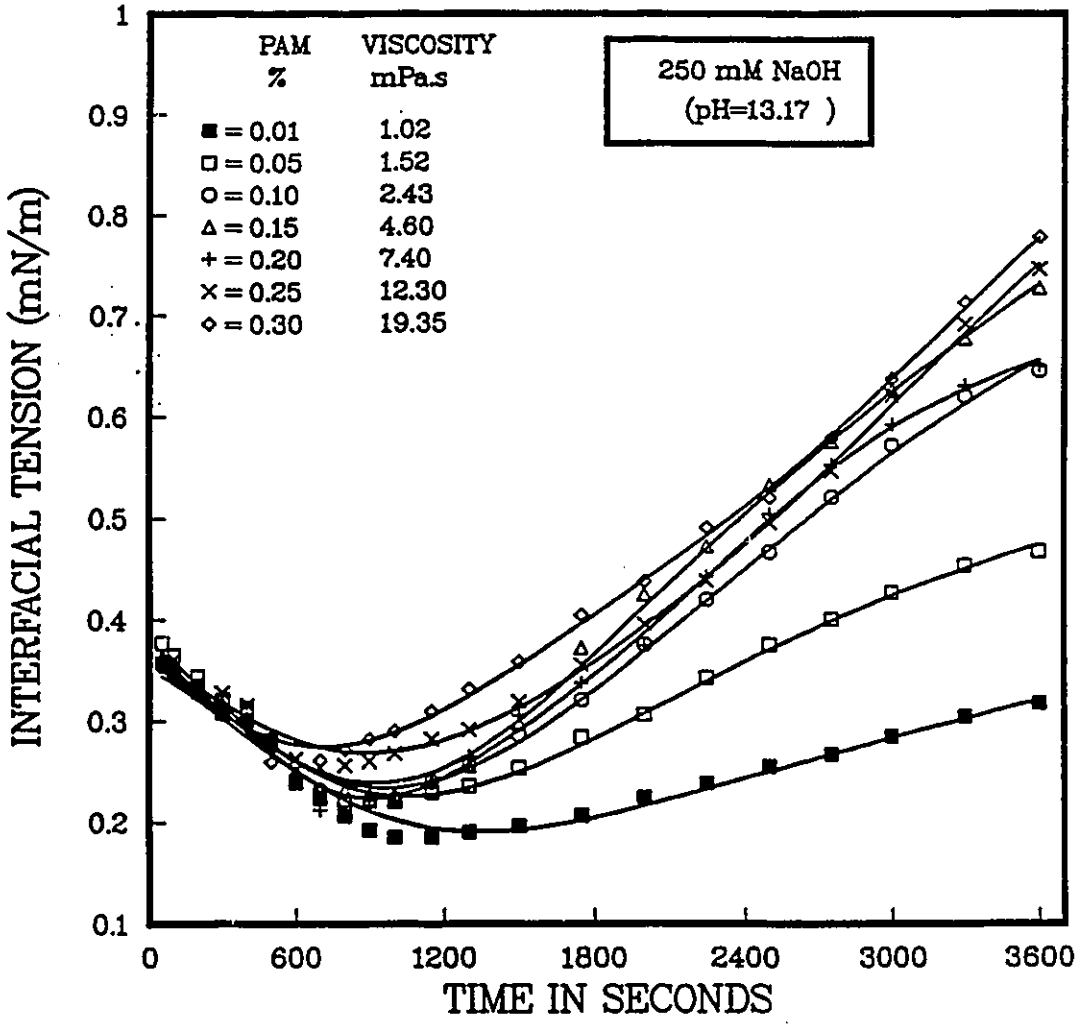

Figure 4.21: Effects of Polyacrylamide (Aqueous Phase viscosity) on Transient IFT behavior of 10 mM Linoleic Acid in Paraffin Oil in contact with 250 mM NaOH Solution at 25° C.

contact times between the polymer/caustic solution with the acidic oil, the excess NaOH hydrolyzed some of the polymer forming additional surface-active polymeric anions. These new surfactants reenforced the previously formed soap anions by the reaction between the caustic and the acid present in the oil. This results then in a favorable interactions between the various surface-active species. However at longer contact times, desorption of the surface-active species away from the interface resulted in a faster increase in IFT. The fact that the IFT values for the polymer/caustic systems were generally higher than the figures obtained when no polymer was added, suggested that the polymeric anions desorbed much faster than the carboxylate anions. Furthermore, it is quite probable that the carboxylate and polymeric anions compete for presence at the oil/water interface. This competition would favor the larger polymeric anions. Thus when these species are removed progressively from the interface, the IFT is bound to rise at a much faster rate.

A comparison of the dynamic IFT data for the two polymers shows that at all NaOH concentrations, the IFT values obtained at longer contact times with PVA were very much higher than corresponding values determined when PAM was used. A probable reason for this behavior may be due to the lower apparent diffusivity of PAM (being a much bigger macromolecule). This lower diffusivity would result in a slower rate of desorptive-diffusion out of the interface. Consequently the IFT would increase at a much slower rate.

4.4 Effects of Oil Phase Viscosity on Dynamic IFT

A study of the effects of oil phase viscosity on dynamic IFT was carried out in a similar way to that described for the aqueous phase. An oil-soluble, water-insoluble additive (viz., polystyrene) was used to enhance the viscosity of the oil phase. In this section Neale et al.'s [10] results were reproduced with the same systems, i.e. for 10 % crude oil dissolved in polystyrene-toluene mixture as shown in Fig. 4.22. Also the IFT for 10 mM linoleic acid dissolved in the latter were measured. Fig. 4.23 depicts such dynamic IFT behavior and shows that this system exhibited the same IFT-time trends that were observed for the toluene diluted crude oil. It was shown [10] that polystyrene is unlikely to significantly alter the IFT because of its relative interfacial insensitivity.

In general, we observed a sharp rise in IFT with extended contact times. The minimum in IFT occurred within the first few seconds of spinning and could not be recorded. Comparing the data presented in Fig. 4.23 with those of Fig. 4.22, we find that the IFT values are lower in the case of the former. The reason for this is because the oil phase contains 10 mM of a single surface-active species (i.e. equivalent to an acid number of 0.56 mg KOH/ g oil) which is much higher than that of the dilute crude oil. It is thus clear from Fig. 4.23 that varying the viscosity of the oil phase has a significant effect on the measured IFT. Thus, an increase

in polystyrene concentration (i.e. increase in oil viscosity) produces a significant decrease in dynamic IFT.

Neale et al [10] opined that increasing the viscosity of the oleic phase affected the rates of elongation and contraction of the spinning droplet, thereby leading to differences in apparent tension values. The effects of viscosity on dynamic IFT can also be viewed as a consequence of the change in mass-transfer resistances due to the change in oil viscosity. From theoretical considerations, it would seem that mass-transfer resistances could significantly inhibit or promote the extraction of acids from the oleic phase. It could also influence the rate of desorption of the surface-active soaps away from the oil-water interface. Several researchers have also shown that the rate of desorption of the surface-active species from the oil-water interface controlled the overall kinetic-diffusive process. Mansfield [80] postulated that a slow diffusion rate in the viscous oil phase could be the governing factor. Mansfield's assertion was confirmed in part by the theoretical and experimental evidence presented by Rubin and Radke [2].

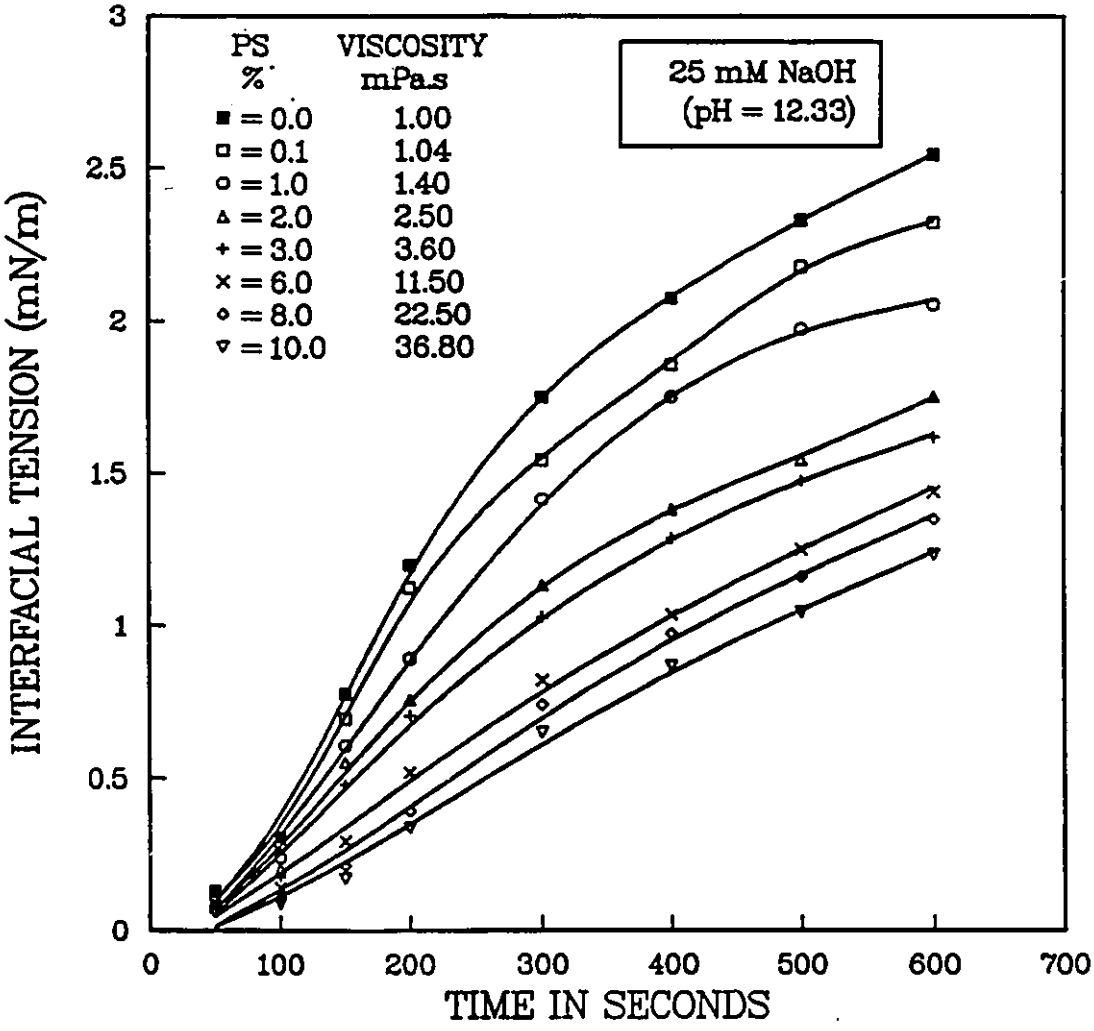

Figure 4.22: Effects of Polystyrene on Transient IFT behavior of 10 % Lloydminster Oil-in-Toluene against an aqueous 25 mM NaOH Solution at 25° C.

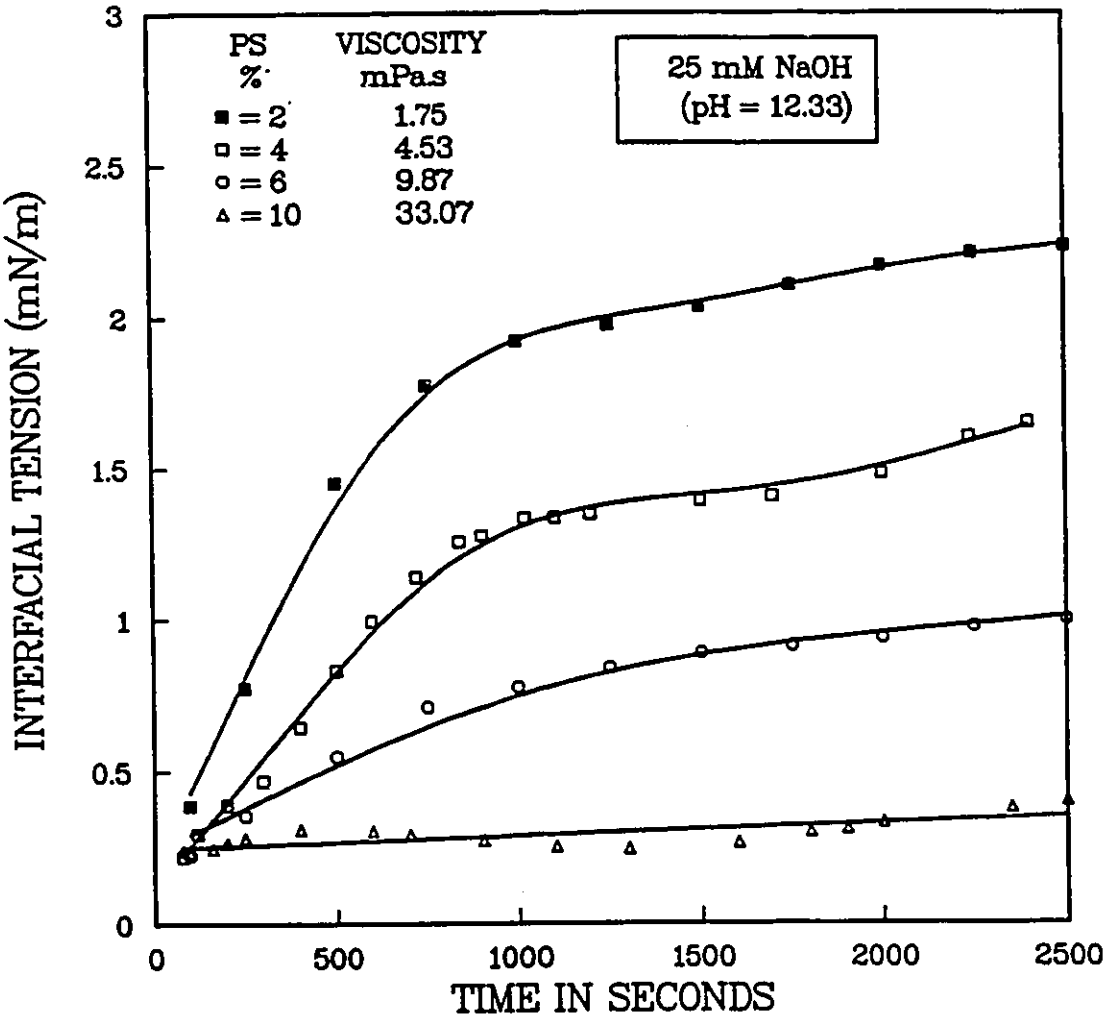

Figure 4.23: Effects of Polystyrene on Transient IFT behavior of 10 mM Linoleic Acid in Toluene against an aqueous 25 mM NaOH Solution at 25° C.

Chapter 5

Conclusions and Recommendations

Conclusions

1. Polyvinyl alcohol and polyacrylamide solutions in water exhibited a non-nNwtonian behavior with viscosity increasing markedly with polymer concentration. The synergistic effects of combining polymers with alkaline solutions did not significantly affect the viscosity behavior.

2. Lloydminster crude oil contacted with 25 mM NaOH exhibited a dynamic IFT behavior with a minimum tension of 0.022 mN/m attained after 400 seconds.

3. Linoleic acid solution in paraffin oil contacted with NaOH solutions exhibited a dynamic IFT trend similar to that obtained for Lloydminster oil. This system showed an increasing interfacial activity with an increase in acid concentration. For 10 mM linoleic acid in paraffin oil, the lowest IFT was obtained

when contacted with 12.5 mM NaOH solution.

4. Polyvinyl alcohol and polyacrylamide solutions were found to possess a limited degree of interfacial activity. However the resulting IFT values decreased only slightly at extended contact times.

5. Polyvinyl alcohol-caustic solutions in contact with 10 mM linoleic acid produced IFT values t generally higher than those obtained with NaOH alone. The IFT trends showed a relatively small minimum near 0.5 mN/m at early contact times followed by a dramatic increase to values near 8 mN/m.

6. With polyacrylamide-caustic systems, a deeper IFT minimum was observed and the increase in IFT at larger contact times was much smaller.

7. The spinning drop tensiometer, despite certain practical limitations, is capable of measuring the dynamic IFT behavior of reacting systems. However, the modified spinning drop tensiometer is experimentally more convenient, and gives better accuracy and precision both for IFT and contact times.

8. The IFT trends exhibited by the polymer/caustic systems are of great significance in the design of mobility controlled caustic systems for heavy oil recovery.

Recommendations

A mechanistic modelling approach could be used to obtain the mass-transfer and sorptive kinetic parameters for these linoleic acid/paraffin oil systems. In addition, data on the adsorption of polymeric molecules at oil-water interfaces and in the presence of caustic would enable the results of the polymer-caustic tension studies to be mechanistically interpreted. Armed with information on the mechanism of hydrolysis, degree of polymerization and phase behavior of the polymers, an attempt could than be made to predict theoretically the extent to which a given polymer would enhance aqueous phase viscosity and the degree of non-Newtonian behavior to be expected.

Bibliography

[1] Sherwood, T.K., and Wei, J.C.:*Interfacial Phenomena in Liquid-Liquid Extraction,* Ind. Eng. Chem., Vol 49, No 6, (Jun 1957), pp 1033–1034.

[2] England, D.C. and Berg, J.C.:*Transfer of Surface-Active Agents across a Liquid-Liquid Interface,* AIChE J., Vol 17, No 2, (Mar 1971), pp 313–322.

[3] Rubin, E. and Radke, C.J.: *Dynamic Interfacial Tension Minima in Finite Systems,* Chem. Eng. Sci., Vol 35, 1980, pp 1129-1138.

[4] Adamson, A.W.:*Physical Chemistry of Surfaces,* 3rd Edition, John Wiley and Sons, New York, 1976.

[5] Davies, J.T., and Rideal, E.K.:*Interfacial Phenomena,* 2nd Edition, Academic Press, New York, 1963.

[6] Tanford, C.:*The Hydrophilic Rffect: Formation of Micells and Biological Membranes,* John Wiley and Sons, N.Y., 1980.

[7] Bashforth, F., and Adams, J.C.:*An Attempt to Test the Theories of Capillary Action,* Cambridge University Press, Cambridge, 1983.

[8] Princen. H.M., Zia, I.Y.Z. and Mason, S.G.:*Measurement of Interfacial tension from the shape of a Rotating Drop,* J. Colloid Interface Sci., Vol 23, 1967, pp 99-107.

[9] Cayias, J.L., Schechter, R.S. and Wade, W.H.:*the Measurement of Low Interfacial Tension via the Spinning Drop Technique, in Adsorption at Interfaces,* ACS Symposium Series, No 8, (mittal, K.L., Editor), Washington D.C., 1975, pp 234-247.

[10] Neale, G.H., Khulbe, K.C and Hornof, V.:*Effects of Oil Phase viscosity on Interfacial Tension Behaviuor of Oil/Alkaline Systems as Measured by the Spinning Drop Tensiometer,* Can. J. Chem. Eng., Vol 62, (Aug 1985),pp 700-705.

[11] Taber, J.J. and Martin, F.D.:*Technical Screening Guides for the Enhanced Recovery of Oil,* SPE 12069, presented at the 58th Annual Conference and Exhibition of the Society of Petroleum Engineers, San Fransisco, California, 1983.

[12] Taber, J.J.:*Research on Enhanced Oil Recovery: Past, Present, and Future,* Pure App. Chem., No 52, (1980),pp 1323–1347.

[13] Jha, K.N.:*Enhanced Oil Recovery: An Introduction,* Chemistry in Canada, No 34, (1982), pp 19–26.

[14] Prince, J.P.:*Enhanced Oil Recovery Potential in Canada – A Methodological Review,* Canadian Energy Research Institute, Calgary, 1978.

[15] Neumann, H.J., Erdol und Kohle, Vol 17, (1964), p 346.

[16] Lochte,H.L.:*Petroleum Acids and Basis,* Ind. Eng. Chem., Vol 44,No 11, (Nov 1952), pp 2597–2601.

[17] Seifert, W.K. , and Howells, W.G.:*Interfacially Active Acids in a California Crude Oil,* Anal. Chem., Vol 41, No 12, (Oct 1969), pp 1638–1647.

[18] Seifert,W.K. and Teeter,R.M.:*Preperative Thin Layer Chromatography and High Resolution Mass Spectrometry of Crude Oil carbaxylic Acids,*

Anal. Chem., Vol 41, No 6, (May 1969), pp 786–795.

[19] Seifert,W.K. and Teeter,R.M.:*Identification of Polycyclic Aromatic and Heterocyclic Crude Oil Carboxylic Acids,* Anal. Chem., Vol 42, No 7, (Jun 1970), pp 750–758.

[20] Seifert,W.K., Gallegos, E.G., and Teeter,R.M.:*Proof of Structure of Steroid Carboxylic Acids in a California Petroleum by Deuterium Labelling, Synthesis and Mass Spectrometry,* J. Am. Chem. Soc., Vol 94, No 16, (Aug 1972), pp 5880–5887.

[21] Jenkins., G.I., J. Inst. Pet., Vol 51, (1965), pp 313-317.

[22] Jang, L.K., Sharma, M.M., Chang, Y.I.,Chan, M., and Yen, T.F.:*Correlation of Petroleum Component Properties for Caustic Flooding,* AIChE Symposium Series, Vol 78, No 212, (1982), pp 97–104.

[23] Sharma, M.M., Jang, L.K., and Yen, T.F.:*Transient Interfacial Tension Behaviour of Crude Oil-Caustic Interfaces,* paper No 12669, presented at the SPE/DOE 4th Symposium on Enhanced Oil Recovery, Tulsa, Oklahoma, (April 15–18, 1984).

[24] Dunning, H.N., Moore, J.W., and Denekas, M.D.:*Interfacial Activities and Porphyrin Contents of Petroleum Extracts,* Ind. Eng. Chem., Vol 45, No 8, (Aug 1953), pp 1759–1765.

[25] Khulbe, K.C., Neale, G.H., and Hornof, V.:*Interfacial Activity of Heavy Oil and Its Maltene Constituents against Caustic Solution,* AOSTRA J. Research, Vol 2, No 2, 1985, pp 95-101.

[26] Ramakrishnan, T.S., and Wasan, D.T.:*A Model for Interfacial Activity of Acidic Crude Oil/Caustic Systems for Alkaline Flooding,* Soc. Pet. Eng. J., (Aug 1983), pp 602–612.

[27] Nutting, P.G.:*Soda Process for Petroleum Recovery,* Oil Gas J., Vol 25, No 45, 76, 150 (1927).

[28] Campbell, T.C.:*The Role of Alkaline Chemicals in Oil Displacement Mechanisms in Surface Phenomena in Enhanced Oil Recovery,* Shah D.O.(Editor), Plenum Press, N.Y., 1981, pp 293-306.

[29] Campbell, T.C.:*The Role of Alkaline Chemicals in the Recovery of Low-Gravity Crude Oils,* J. Pet. Tech., (Nov 1982), pp 2510–2516.

[30] Cooke,C.E..Jr, Williams,R.E. and Kolodzie,P.A:*Oil Recovery by Alkaline Waterflooding,* J. Pet. Tech., (Dec 1974), pp 1365–1374.

[31] McCaffery,F.G.:*Interfacial Tensions and Aging Behaviour of some Crude Oils against Caustic Solutions,* J. Can. Pet. Eng.,(Aug 1983), pp 645–656.

[32] deZabala,E.F. and Radke,C.J.:*The role of Interfacial Resistances in Alkaline Waterflooding of Acid Oils,* SPE paper No 11213, presented at the 57th Annual Fall Technical Conference of AIME, New Orleans, LA, Sept 26-29, 11982.

[33] Atkinson, H.:*Recovery of Petroleum from Oil Bearing Sands,* U.S. Patent No 1,651,311 (1927).

[34] Subkow,P.:*Process for the Removal of Bitumen from Bituminous Deposits,* U.S. Patent No 2,288,857, (Jul 7,1942).

[35] Johnson,C.E.:*Status Of Caustic and Emulsion Methods,* J. Pet. Tech., (Jan 1976), pp 85–92.

[36] Owens, W.W., and Archer, D.L.,:*The Effect of Rock Wettability on Oil-Water Relative Permeability Relationships,* J. Pet. Tech., (July 1971), pp 873–878.

[37] Wagner,O.R. and Leach,R.O.:*Improving Oil Displacement Effiency by Wettability Adjustment,* AIME Pet. Trans., Vol 216,(1956),pp 63–72.

[38] Ehrlich, R., Hasiba, H.H., and Raimond, P.:*Alkaline Waterflooding for Wettability Alteration- Evaluation of Potential Field Application,* J. Pet. Tech., (Dec 1974), pp 1335–1343.

[39] Jennings,H.Y.,Johnson,C.E.Jr and McAuliffe,C.D.:*A Caustic Waterflooding Process for Heavy Oils,* J. Pet. Tech., (Dec 1974),pp 1365–1374.

[40] Castor,T.P., Somerton,W.H. and Kelly,J.F.:*Recovery Mechanisms of Alkaline Flooding, in Surface Phenomena in Enhanced Oil Recovery,* Shah,D.O.(Editor), Plenum Press,N.Y., 1981, pp 249-291.

[41] Alam, M.W, and Tiab, D.:*Mobility Control of Caustic Flood,* Energy Sources, Vol 10, (1988), pp 1–19.

[42] Potts, D.E., and Kuehne, D.L.:*Strategy for Alkaline/Polymer Flood Design with Berea and Reservoir-Rock Corefloods,* SPE Reservoir Eng., (Nov 1988), pp 1143–1152.

[43] Shuler, P.J., Kuehne, D.L., and Lerner, R.M.:*Improving Chemical Flood Efficiency with Micellar/Alkaline/Polymer Processes,* J. Pet. Tech., (Jan 1989), pp 80–88

[44] Shupe, R.D.:*Chemical Stability of Polyacrylamide Polymers,* J. Pet. Tech., Vol 33, (August 1981), pp 1513–1529.

[45] Flory, P.J.:*Principles of Polymers Chemstry,* Cornell University Press, Ithaca, N.Y., 1953.

[46] Rodriguez, F.:*Principles of Polymers Systems*, 2nd Edition, McGraw Hill, N.Y., 1982.

[47] Krumrine, P.H., and Falcone, J.S.Jr.:*Surfactant, Polymers and Alkali Interactions in Chemical Flooding Processes,* paper SPE 11778, presented at the 1983 SPE Intl. Symposium on Oilfield and Geothermal Chemistry, Denver, (June 1-3, 1983).

[48] Mungan, N.:*Improved Waterflooding through Mobility Control,* Can. J. Chem. Eng., Vol 49, (Feb 1971), pp 32–37.

[49] Ryles, R.G.:*Chemical Stability Limits of Water-Soluble Polymers Used in Oil Recovery Processes,* paper SPE 13585, presented at the 1985 SPE Intl. Symposium on Oilfield and Geothermal Chemistry, Phoenix, Arizona, (April 9-11, 1985).

[50] Chan, M.S.:*Determination of Electrophoretic Mobility and Related Interfacial Properties for Crude Oil Emulsions,* M.S. Thesis, Illinois Inst. Technology, Chigago (1978).

[51] Chan,M. and Yen,T.F.:*A Chemical Equilibrium Model for Interfacial Activity of Crude Oil in Aqueous Alkaline Solution: The Effect of pH, Alkali and Salt,* Can. J. Chem. Eng., Vol 60, (April 1982),pp 305-308.

[52] Sharma,M.M. and Yen,T.F.:*A Thermodynamic Model for Low Interfacial Tensions in Alkaline Flooding,* Soc. Pet. Eng. J.,(Feb 1983), pp 125–134.

[53] Trujillo, E.M.:*The Static and Dynamic Interfacial Tensions between Crude Oil and Caustic Solutions,* Soc. Pet. Engrs. J., 23, (Aug 1983), pp 645–656.

[54] Borwankar, R.P., and Wasan, D.T.:*Dynamic Interfacial Tension in Acidic Crude Oil/Caustic Systems Part I: A Chemical Diffusion-Kinetic Model,* AIChE J., Vol 32,No 3, (March 1986), pp 455–466.

[55] Borwankar, R.P., and Wasan, D.T.:*Dynamic Interfacial Tension in Acidic Crude Oil/Caustic Systems Part II: Role of Dynamic Effects in Alkaline Flooding For Enhanced Oil Recovery,* AIChE J., Vol 32,No 3, (March 1986), pp 467–476.

[56] Chiwetelu, C.I.:*Dynamic Intefacial Tension of Finite Reactive Systems Related to Enhanced Oil Recovery,* Ph.D. Thesis, University of Ottawa, Ottawa, 1987.

[57] Clift, R., and Weber, M.E.:*Bubbles, Drops and Particles,* Academic Press, New York, 1978.

[58] Sawistowski, H.:*Recent Advances in Liquid-Liquid Extraction,* (C. Hansen, Ed.), Pergamon, Oxford, 1971.

[59] Sternling, C.V., and Scriven, L.E.:*Interfacial Turbulence: Hydrodynamic Instability and Marangoni Effect,* AIChE J., Vol 5, No 4, (Dec 1959), pp 514–523.

[60] Brown, J.B. and Radke, J.C.: *Area Effects in Spinning drop Dynamic Interfacial Tensions,* Chem. Eng. Sci., Vol 35, 1980, pp 1458-1460.

[61] deZabala,E.F., and Radke,C.J.:*The Role of Interfacial Resistances in Alkaline Waterflooding of Acid Oils,* SPE paper No 11213, presented at the 57th Annual Fall Technical Conference of SPE of AIME, New Orleans, LA, Sept 26–29, 1982.

[62] deZabala,E.F.:*Tertiary Recovery of Acidic Crudes from Oilsands. Mechanisms and Modelling,* Ph.D Thesis, University of California, Berkeley,1984.

[63] Bansal,V.K., Chan,K.S., McCallough,R. and Shah,D.O.:*The effect of Caustic Concentration on Interfacial Charge, Interfacial Tension and*

Droplet Size, a Simple Test for Optimum Caustic Concentration for Crude Oils, J. Can. Pet. Tech., (Jan-Mar 1978), pp 69–72.

[64] Currie, P.K., and van Nieuwkoop, J.:*Buoyancy Effects in the Spinning-Drop Interfacial Tensiometer,* J. Colloid Interface Sci. , Vol 87, No 2, (1982), pp 301–316.

[65] Manning, C.D., and Scriven, L.E.:*Interfacial Tension Measurement with a Spinning Drop in Gyrostatic Equilibrium,* J. Can. Pet. Tech., Vol 15, No 3, (1976), 71.

[66] Chiewetelu, I.C., Hornof, V., and Neale, H.G.: *The Measurement of Dynamic Interfacial Tension by Photo-Micropendography,* J. Colloid Interface Sci., Vol 125, No 2 (Oct 1988), pp 586–601.

[67] Chatenay, D., Langevin, D., and Meunier, J.:*Measurement of Low Interfacial Tension, Comparison between a Light Scattering Technique and the Spinning Drop Technique,* J. Dispersion Sci., Vol 3, No 3 (1982), pp 245–260.

[68] Gardner, J.E., and Hayes, M.E.:*University of Texas Model 500 Spinning-Drop Tensiometer Instruction Manual.*

[69] Reive, D.M.:*Interfacial Tension Behaviour of a Canadian Heavy Oil against Caustic Solutions,* M.A.Sc. Thesis, University of Ottawa, Ottawa, 1985.

[70] Chiwetelu, C.I., Neale, G.H, and Hornof, V.:*The Measurement of Dynamic Interfacial Tension by Spinning Drop Photo-Tensiometry,* Rev. Sci. Instrum. (Submitted June 1989).

[71] Slattery, J.C. and Chen, J.D.:*Alternative Solution for Spinning Drop Interfacial Tensiometer,* J. Colloid Interface Sci., Vol 64, No 2, (April 1978), pp 371-373.

[72] Harkins, W.D., and Jordan, H.F., J. Am. Chem. Soc., Vol 52, (1930), 1751.

[73] Davidson, R.L.:*Handbook of Water-Soluble Gums and Resins,*, (Editor), McGraw-Hill, 1980.

[74] Babu, D.R., Hornof, V., and Neale, G.H.:*Evaluation of Aqueous Chemical Systems for Heavy Oil Recovery Processes,* Fuel, Vol 65, (Jan 1986), pp 4-7.

[75] Mode, T.W.:*Polyvinyl Alcohol,* Chapter 20 in Ref [73], pp 20.1–20.32.

[76] Volk, H., and Friedrich, R.E.:*Polyacrylamide,* Chapter 16 in Ref [73], pp 16.1–16.26.

[77] Finch, C.A.:*Polyvinyl Alcohol Properties and Applications,* John Wiley and Sons, N.Y., (1973).

[78] Pritchand, J.C.:*Poly(Vinyl Alcohol) Basic Properties and Uses,* Gordan and Breach, Sci. Publishers, N.Y., (1970).

[79] Danielli, J.F., Pankhurt, K.G.A., and Riddifort, A.C.:*Surface Phenomena in Chemistry and Biology,* Pergamon. N.Y., (1958).

[80] Mansfield, W.W, Aut. J. Sci. Res., A5 (1952), p 331.

Appendix A

Physical Properties of Solutions

Table A1: Density of Polyvinyl Alcohol-Caustic Solutions at 25° C (kg/m^3)

System	CAUSTIC CONCENTRATION					
Polymer wt %	0.0 mM	2.5 mM	12.5 mM	25 mM	125 mM	250 mM
0.00	997.0461	997.1589	997.6001	998.0583	1002.5142	1007.6536
0.30	997.7131	997.8225	998.2634	998.7078	1003.1179	1008.2573
0.60	998.3801	998.4863	998.9268	999.3572	1003.7217	1008.8613
0.90	999.0471	999.1501	999.5901	1000.0068	1004.3257	1009.4653
1.20	999.7141	999.8140	1000.2534	1000.6562	1004.9294	1010.0693
1.50	1000.3811	1000.4775	1000.9167	1001.3059	1005.5334	1010.6733
1.80	1001.0481	1001.1414	1001.5801	1001.9553	1006.1372	1011.2773
2.10	1001.7151	1001.8052	1002.2437	1002.6050	1006.7412	1011.8813
2.40	1002.3821	1002.4690	1002.9070	1003.2544	1007.3450	1012.4854
2.70	1003.0491	1003.1326	1003.5703	1003.9041	1007.9490	1013.0894
3.00	1003.7161	1003.7964	1004.2336	1004.5535	1008.5527	1013.6934

Table A2: Density of Polyacrylamide-Caustic Solutions at 25° C (kg/m^3)

System	CAUSTIC CONCENTRATION					
Polymer wt %	0.0 mM	2.5 mM	12.5 mM	25 mM	125 mM	250 mM
0.00	997.0461	997.1589	997.5989	998.1431	1002.4565	1007.6445
0.01	997.1047	997.1902	997.6301	998.1743	1002.4727	1007.6660
0.05	997.2393	997.3162	997.7561	998.3003	1002.5378	1007.7522
0.10	997.4072	997.4736	997.9136	998.4578	1002.6191	1007.8599
0.15	997.5752	997.6311	998.0710	998.6152	1002.7007	1007.9675
0.20	997.7432	997.7886	998.2285	998.7727	1002.7820	1008.0752
0.25	997.9111	997.9460	998.3860	998.9302	1002.8633	1008.1829
0.30	998.0791	998.1035	998.5435	999.0876	1002.9448	1008.2905

Table A3: pH of Polyvinyl Alcohol-Caustic Solutions at 25° C

System	CAUSTIC CONCENTRATION					
Polymer wt %	0.0 mM	2.5 mM	12.5 mM	25 mM	125 mM	250 mM
0.00	7.03	11.38	12.05	12.32	12.97	13.19
0.30	6.92	11.30	12.00	12.28	12.92	13.17
0.60	6.56	11.30	12.00	12.28	12.91	13.15
0.90	6.60	11.28	11.98	12.27	12.92	13.14
1.20	6.62	11.26	11.97	12.25	12.90	13.14
1.50	6.54	11.26	11.97	12.24	12.86	13.12
1.80	6.58	11.24	11.95	12.22	12.86	13.10
2.10	6.57	11.21	11.94	12.20	12.79	13.08
2.40	6.49	11.20	11.92	12.20	12.75	13.07
2.70	6.68	11.18	11.90	12.18	12.73	13.07
3.00	6.51	11.17	11.89	12.15	12.71	13.05

Table A4: pH of Polyacrylamide-Caustic Solutions at 25° C

System	CAUSTIC CONCENTRATION					
Polymer wt %	0.0 mM	2.5 mM	12.5 mM	25 mM	125 mM	250 mM
0.00	7.00	11.40	12.09	12.34	12.97	13.19
0.01	7.97	11.36	12.05	12.32	12.90	13.15
0.05	6.95	11.36	12.03	12.33	12.89	13.13
0.10	6.93	11.35	12.00	12.31	12.88	13.13
0.15	6.91	11.29	12.00	12.31	12.89	13.13
0.20	6.88	11.22	11.95	12.31	12.89	13.12
0.25	6.86	11.18	11.95	12.30	12.85	13.11
0.30	6.82	11.17	11.94	12.30	12.87	13.10

Table A5: Viscosity of Polyvinyl Alcohol-Caustic Solutions (mPa.s) at 12 rpm and 25° C

System	CAUSTIC CONCENTRATION					
Polymer wt %	0.0 mM	2.5 mM	12.5 mM	25 mM	125 mM	250 mM
0.0	1.00	1.00	1.00	1.00	1.00	1.00
0.3	1.65	1.62	1.59	1.50	1.45	1.48
0.6	2.50	2.45	2.41	2.31	2.22	2.17
0.9	3.52	3.48	3.36	3.26	3.20	3.14
1.2	4.48	4.42	4.36	4.31	4.22	4.12
1.5	6.15	6.11	6.06	5.94	5.88	5.76
1.8	8.25	8.17	8.12	7.98	7.83	7.80
2.1	11.0	11.0	10.9	10.8	10.71	10.65
2.4	15.1	15.1	15.0	14.8	14.70	14.62
2.7	20.5	20.5	20.1	19.8	19.40	19.28
3.0	28.0	28.0	27.5	26.4	25.70	25.4

Table A6: Viscosity of Polyacrylamide-Caustic Solutions (mPa.s) at 12 rpm and 25° C

System	CAUSTIC CONCENTRATION					
Polymer wt %	0.0 mM	2.5 mM	12.5 mM	25 mM	125 mM	250 mM
0.00	1.00	1.00	1.00	1.00	1.00	1.00
0.01	1.25	1.25	1.20	1.18	1.08	1.02
0.05	1.90	1.82	1.78	1.72	1.65	1.52
0.10	2.80	1.80	2.74	2.67	2.52	2.43
0.15	4.95	4.90	4.86	4.82	4.71	4.60
0.20	7.90	7.90	7.81	7.75	7.60	7.40
0.25	13.0	12.92	12.78	12.60	12.48	12.30
0.30	21.1	20.80	20.30	19.8	19.50	19.35

Table A7: Viscosity of Polyvinyl Alcohol-Caustic Solutions (mPa.s) at different rpm and 25° C

System	CAUSTIC CONCENTRATION											
olymer	0 mM				25 mM				250 mM			
%	6 rpm	12 rpm	30 rpm	60 rpm	6 rpm	12 rpm	30 rpm	60 rpm	6 rpm	12 rpm	30 rpm	60 rpm
0.6	2.60	2.50	1.90	1.10	2.50	2.40	1.80	1.10	2.25	2.17	1.70	1.35
1.2	4.76	4.48	4.00	2.50	4.40	4.31	3.92	3.33	4.18	4.12	3.72	3.15
1.8	8.60	8.25	7.35	5.20	8.12	7.98	6.88	6.17	7.97	7.80	6.42	5.88
2.4	15.5	15.1	14.0	–	14.9	14.8	13.7	–	14.8	14.6	13.2	–
3.0	28.4	28.0	–	–	26.7	26.4	–	–	25.7	25.4	–	–

Table A8: Viscosity of Polyacrylamide-Caustic Solutions (mPa.s) at different rpm and 25° C

System	CAUSTIC CONCENTRATION											
olymer	0.0 mM				25 mM				250 mM			
%	6 rpm	12 rpm	30 rpm	60 rpm	6 rpm	12 rpm	30 rpm	60 rpm	6 rpm	12 rpm	30 rpm	60 rpm
0.05	1.95	1.90	1.70	1.33	1.84	1.78	1.52	1.21	1.54	1.52	1.20	1.11
0.15	5.08	4.95	4.42	3.60	4.93	4.82	4.33	3.45	4.67	4.60	3.96	3.50
0.25	13.10	13.00	11.90	–	12.70	12.60	11.72	–	12.37	12.30	11.80	–
0.30	21.40	21.10	–	–	20.20	19.80	–	–	19.70	19.35	–	–

Table A.9: Physical Properties of Oleic Solutions at 25° C

Identification	Density (kg/m^3)	Viscosity (mPa. s)
Lloydminster Crude Oil	970.500	—
10 % Crude Oil-in-Toluene		
0 % Polystyrene	858.0	1.00
2 % polystyrene	862.0	2.50
4 % Polystyrene	867.0	5.57
6 % Polystyrene	871.9	11.5
8 % Polystyrene	876.9	22.5
10 % Polystyrene	881.9	36.8
10 mM Linoleic Acid-in-Toluene		
0 % Polystyrene	857.0	1.00
2 % Polystyrene	860.8	1.75
4 % Polystyrene	866.2	4.53
6 % Polystyrene	870.4	9.87
8 % Polystyrene	875.7	20.45
10 % Polystyrene	880.7	33.07
Light Paraffin Oil	838.80	19.260
1 mM HL in Paraffin Oil	838.813	19.451
10 mM HL in Paraffin Oil	839.025	19.766
20 mM HL in Paraffin Oil	839.236	19.786
100 mM HL in Paraffin Oil	840.930	19.821